applied sciences

MDPI

Review

Emergence of White Organic Light-Emitting Diodes Based on Thermally Activated Delayed Fluorescence

Peng Xiao [1], Ting Dong [2], Jianing Xie [1,*], Dongxiang Luo [3], Jian Yuan [1] and Baiquan Liu [4,5,*]

1 School of Physics and Optoelectronic Engineering, Foshan University, Foshan 528000, China; xiaopeng@fosu.edu.cn (P.X.); yuanjian054@163.com (J.Y.)
2 Guangdong Juhua Printed Display Technology Co. Ltd. Guangzhou 510006, China; dongt@tcl.com
3 School of Materials and Energy, Guangdong University of Technology, Guangzhou 510006, China; luodx@gdut.edu.cn
4 Institute of Polymer Optoelectronic Materials and Devices, State Key Laboratory of Luminescent Materials and Devices, South China University of Technology, Guangzhou 510640, China
5 LUMINOUS! Center of Excellence for Semiconductor Lighting and Displays, School of Electrical and Electronic Engineering, Nanyang Technological University, Nanyang Avenue, Singapore 639798, Singapore
* Correspondence: xiejianingfs@126.com (J.X.); bqliu@ntu.edu.sg (B.L.)

Received: 16 January 2018; Accepted: 13 February 2018; Published: 19 February 2018

Abstract: Recently, thermally activated delayed fluorescence (TADF) organic light-emitting diodes (OLEDs) have attracted both academic and industrial interest due to their extraordinary characteristics, such as high efficiency, low driving voltage, bright luminance, lower power consumption and potentially long lifetime. In this invited review, the fundamental concepts of TADF have been firstly introduced. Then, main approaches to realize WOLEDs based on TADF have been summarized. More specifically, the recent development of WOLEDs based on all TADF emitters, WOLEDs based on TADF and conventional fluorescence emitters, hybrid WOLEDs based on blue TADF and phosphorescence emitters and WOLEDs based on TADF exciplex host and phosphorescence dopants is highlighted. In particular, design strategies, device structures, working mechanisms and electroluminescent processes of the representative WOLEDs based on TADF are reviewed. Finally, challenges and opportunities for further enhancement of the performance of WOLEDs based on TADF are presented.

Keywords: white; organic light-emitting diodes; thermally activated delayed fluorescence; charge; exciton

1. Introduction

Luminescence is a type of cold body radiation caused by external stimuli, such as electric field, mechanical stress, photoabsorption and chemical reactions [1–6]. For the electroluminescence, it is referred to the process that holes and electrons are recombined to furnish light. In 1953, Bernanose et al. first discovered organic materials to produce electroluminescence, by using a cellulose film doped with acridine orange [7]. In 1963, Pope et al. achieved the electroluminescence by utilizing an anthracene single crystal connected to high-field carrier injection electrodes [8]. Since then, there is an increasing interest for the electroluminescence of organic materials. In 1987, Tang et al. reported the first organic light-emitting diode (OLED) [9]. In their device, charges of both polarities were injected into the organic layers and the subsequent charge transport and recombination produced green emission originating from singlet excitons; that is, fluorescence. In general, OLEDs possess many outstanding characteristics, such as high efficiency, low power consumption, fast switching, wide viewing angle, light weight, long lifetime and flexibility [10–12].

After the invention of OLED, other kinds of LEDs (e.g., polymer LED, quantum-dot LED, nanoplatelet LED and perovskite LED) were also successively reported [13–19]. By dint of the strategies used in OLEDs, the performance of other kinds of LEDs can be greatly enhanced. Besides, with the increasingly

understanding the insight of OLEDs, the concepts utilized in OLEDs can also be applied to other optoelectrical devices, which is beneficial to the development of related fields [20–23].

Nowadays, the OLED field has evolved to the extent that commercial applications for cell-phones, televisions and lamps are available. Furthermore, to satisfy the requirements of energy-saving lighting and high-quality displays, attentions have been gradually paid on the white OLED (WOLED) technology [24–30]. In 1994, Kido et al. made the pioneer works of WOLEDs [31,32]. Over the past two decades, the power efficiency (PE) of WOLEDs has been improved from 0.83 lm W^{-1} to >100 lm W^{-1} [33–36], demonstrating the great potential of WOLEDs for the lighting and displays. In the case of lighting applications, WOLEDs should meet the demand of bright luminance, high efficiency and long lifetime simultaneously. More specifically, WOLEDs require standard fluorescent tube efficiency (40–70 lm W^{-1}) and ≥10,000 h of lifetime at the luminance of ≥1000 cd m^{-2} [24–30]. Besides, the color rendering index (CRI) above 80 is required for the indoor lighting and the Commission International de L'Eclairage (CIE) chromaticity coordinates of WOLEDs should be located near white light equal-energy point (0.33, 0.33). Moreover, for the high-quality lighting, other characterization parameters (e.g., correlated color temperature (CCT), color stability and driving voltage) of WOLEDs are also needed to be taken into account [37–41].

Based on the adopted emissive organic materials, WOLEDs can be fabricated by using fluorescence, phosphorescence and thermally activated delayed fluorescence (TADF) materials [42]. Particularly, the TADF material has been considered as the third-generation OLED emitter after Adachi et al. made a breakthrough on it in 2012 [43–45]. For the conventional fluorescent emitters, only the singlet excitons (25%) can emit light since the radiative decay of triplet excitons (75%) is spin forbidden. In the case of the TADF emitter, it could harness both singlet and triplet excitons since triplets can be harvested as delayed fluorescence through their up-conversion from a lowest triplet state to a lowest singlet state by inducing efficient reverse intersystem crossing (RISC) [46–50]. Therefore, similar to phosphorescence emitters, a maximum internal quantum efficiency (IQE) of 100% can be realized [51–54]. Due to the excellent properties (e.g., noble metal-free characteristic, high efficiency, low driving voltage, bright luminance, lower power consumption and potentially long lifetime), TADF emitters have been actively investigated to develop WOLEDs [42]. Hence, despite the WOLEDs based on TADF just reported in recent years, their performance has been step-by-step improved [55]. To date, WOLEDs based on TADF emitters can exhibit nearly 20% external quantum efficiency (EQE) [56], which is comparable to state-of-the-art phosphorescence WOLEDs [57–59] and fluorescence/phosphorescence hybrid WOLEDs [60–66]. Thus, WOLEDs based on TADF have great potential to the lighting and display field.

Herein, we have first introduced the fundamental concepts of TADF, which are beneficial to comprehend WOLEDs based on TADF. Then, we have summarized main approaches to realize WOLEDs based on TADF. More specifically, we have highlighted the recent development of WOLEDs based on all TADF emitters, WOLEDs based on TADF and conventional fluorescence emitters, hybrid WOLEDs based on blue TADF and phosphorescence emitters and WOLEDs based on TADF exciplex host and phosphorescence dopants. In particular, we have reviewed design strategies, device structures, working mechanisms and electroluminescent processes of the representative WOLEDs based on TADF. Finally, we have presented challenges and opportunities for further enhancement of the performance of WOLEDs with TADF-based on TADF.

2. Fundamental Concepts of TADF

2.1. The Evolution of OLED Emitters

Due to the effect of spin statistics, when holes injected from the anode meet electrons injected from the cathode, singlet and triplet excitons will be formed with a ratio of 1:3 [67–69]. The singlet excitons produced decay rapidly, yielding prompt electroluminescence (fluorescence with lifetimes in nanoseconds). For conventional fluorescent materials, only the singlet excitons (25%) can emit

light since the radiative decay of triplet excitons (75%) is spin forbidden [70–73], as shown in Figure 1a. The conventional fluorescent material is also called the first-generation OLED emitter. By using this kind of emitters, the EQE of fluorescence WOLEDs is usually below 5%, considering that the outcoupling factor is ~20%. In 1998, Ma et al. first demonstrated electron-generated phosphorescence from heavy-metal osmium(II) complexes [74]. In the same year, Baldo et al. reported high-efficiency OLED by using a heavy-metal platinum(II) complex of PtOEP as the phosphor dopant [75]. For the phosphorescent emitter (direct radiative decay of triplet excitons results in phosphorescence with lifetimes in the microsecond to second regime), it can not only harvest triplets via the triplet-triplet energy transfer but also harvest singlets via the singlet-triplet ISC due to the heavy-atom effect, leading to a maximum IQE of 100% [76–79], as shown in Figure 1b. The phosphorescent material is usually referred as the second-generation OLED emitter. By using this kind of emitters, the EQE of phosphorescence WOLEDs can be as high as 20%.

In terms of the TADF material (the third-generation OLED emitter), a small energy gap (ΔE_{ST}) between singlet (S_1) and triplet (T_1) excited states is required and can be attained by carefully designing organic molecules [43]. Generally, the S_1 level is considerably higher in energy than the T_1 level by 0.5–1.0 eV, because of the electron exchange energy between these levels [60]. However, to enhance thermal up-conversion (i.e., $T_1 \rightarrow S_1$ RISC), the molecular design of TADF materials requires small ΔE_{ST}, typically less than 0.2 eV, to overcome competitive non-radiative decay pathways, leading to highly luminescent TADF materials [80]. In addition, to enhance the photoluminescence efficiency of TADF materials, the geometrical change in molecular conformation between its ground state (S_0) and S_1 states should be restrained to suppress non-radiative decay. In TADF emitters, triplets are harvested as delayed fluorescence through RISC, as shown in Figure 1c. As a result, the maximum theoretical IQE of TADF emitters can be 100%. On the other hand, although triplet-triplet annihilation (TTA) makes dark triplet states accessible to emit p-type delayed fluorescence, the maximum theoretical IQE of TTA emitter is only 62.5% [81–84], as shown in Figure 1d. As a result, the further development of TTA emitter may be limited. Herein, we mainly focused on the TADF emitters. By virtue of TADF, the IQE of WOLEDs is possible to be 100%.

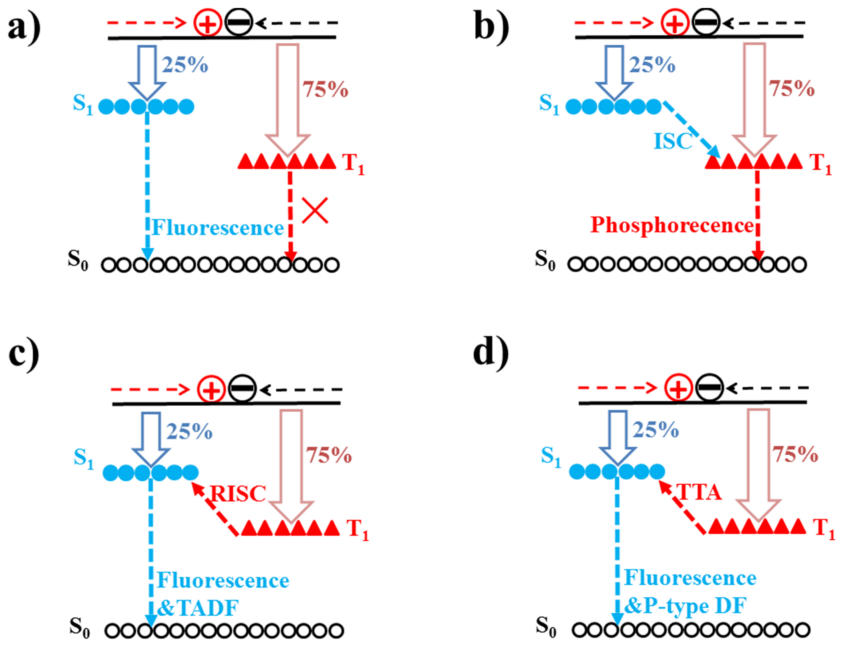

Figure 1. Exciton energy diagram and the possible decay ways of singlet and triplet excitons. Emissions from conventional fluorescent emitters (**a**); phosphorescent emitters (**b**); TADF emitters(**c**) and TTA based emitters (**d**). Reproduced with permission from [42].

2.2. Types of TADF Emitters

In 1961, Paker et al. first discovered purely organic TADF in the eosin dye, which is named as E-type delayed fluorescence previously [85]. Then, TADF phenomena in metal-containing material Cu(I)-complex [86] or fullerenes [87] were observed. In 2009, Endo et al. applied TADF materials in OLEDs but the performance is very poor [88]. Only after the breakthrough made by Adachi et al. in 2012 [43], TADF-based OLEDs rapidly grow. So far, the highest EQE of green TADF OLEDs can be >30%, clearly breaking the efficiency limitation of conventional fluorescence OLEDs and is comparable to the rare metal-complex phosphorescence OLEDs [89,90]. In general, there are two distinct unimolecular mechanisms for TADF: promote and delayed fluorescence. For the promote fluorescence, the emission occurs almost immediately after the excitation with a fast decay from the S_1 to S_0 state (within several nanoseconds). In the case of delayed fluorescence, triplets have to be converted into luminescent singlets for the promote fluorescence process via RISC, resulting in an increased fluorescent lifetime up to several microseconds.

For TADF emitters, TADF emissions can be observed from fullerenes or metal-organic complexes, such as Cu(I), Ag(I), Au(I) and Sn(IV) Complexes [91–93]. However, they are usually not efficient for OLEDs. Hence, recent attentions are mostly paid on D-A molecular systems in OLEDs, since D-A molecular systems with pronounced intra/inter-molecular charge transfer character are very suitable to realize small ΔE_{ST} through separated highest occupied molecular orbital (HOMO) and lowest unoccupied molecular orbital (LUMO) for TADF emission [89]. On one hand, in the intramolecular D-A structure (known as TADF material), a donor and an acceptor are connected by a suitable bridge to form a D-A molecule. On the other hand, the intermolecular D-A structure is formed between electron-donating and electron-accepting molecules via charge transfer under electrical excitation (known as TADF exciplex) [94–96]. By codoping in one layer or depositing the two kinds of materials sequentially, the exciplex emission can be formed [97–99]. To achieve efficient TADF exciplex, some requirements are needed: (i) Electron-donating and -accepting molecules should have high T_1, confining the triplet exciplex state to prevent the quenching of the triplet state via the triplet energy back transfer to the donor or acceptor; (ii) shallow HOMO in donor molecules, deep LUMO in acceptor molecules and high photoluminescence efficiency are significant [94]. Generally, both TADF materials and TADF exciplexes can be applied to WOLEDs.

3. Approaches for WOLEDs Based on TADF

3.1. Basic Aspects of WOLEDs Based on TADF

TADF emitters can be used to develop high-performance WOLEDs, because TADF emitters can (i) harness triplet excitons; (ii) exhibit excellent efficiency; (iii) show usually broad emission spectra with rather large full width at half-maximum of about 100 nm, which is wider than that of conventional fluorescent materials due to their charge-transfer nature [100–102]. For WOLEDs based on TADF, apart from the selection of excellent emitters, the careful manipulation of device engineering also plays a significant role in the performance [103–106]. Therefore, to attain the high performance, the design strategies, device structures, working mechanisms and electroluminescent processes of the WOLEDs based on TADF should be well manipulated [107–109]. For example, unlike conventional fluorescence emitters, the T_1 of TADF emitters is necessary to be considered when designing a WOLED architecture, since hosts or nearby layers with low T_1 would quench the triplet excitons, which leads to the low efficiency [110–112]. Besides, the location of TADF emitters is needed to be investigated, since the energy transfer would occur between the contacted different emitters (e.g., energy can transfer from high-energy TADF emitters to low-energy emitters) [113–115]. With the step-by-step understanding of the insight of TADF, various approaches have been reported to develop WOLEDs based on TADF, including the exploitation of all TADF emitters, the combination of TADF and conventional fluorescence emitters, the mixture of blue TADF and phosphorescence emitters and introduction of TADF exciplex host and phosphorescence dopants.

3.2. WOLEDs Based on All TADF Emitters

3.2.1. WOLEDs with Conventional Fluorescent Hosts and all TADF Materials

To realize WOLEDs based on all TADF emitters, the most directed way is the use of conventional fluorescent hosts and all TADF materials. For this way, all blue, green and red emitters are TADF materials. Besides, the conventional fluorescent host should possess high T_1, particularly higher than the blue TADF materials. Otherwise, the triplet excitons of emitters would be quenched by the host, resulting in low performance. Moreover, high-T_1 charge transport materials should be selected, confining the triplet excitons [116–118].

In 2014, Adachi et al. used this approach to realize high-efficiency TADF WOLED [46]. Figure 2 depicts the device structure: ITO/1,4,5,8,9,11-hexaazatriphenylene hexacarbonitrile (HAT-CN, 10 nm)/9,9′,9′′-triphenyl-9H,9′H,9′′H-3,3′:6′,3′′-tercarbazole (Tris-PCz, 35 nm)/10 wt. % 1,2,3,4-tetrakis(carbazol-9-yl)-5,6-dicyanobenzene (4CzPN): 3,3-Di(9H-carbazol-9-yl)biphenyl (mCBP, green EML) (x nm)/6 wt. % 4CzPN: 2 wt. % 41,4-dicyano-2,3,5,6-tetrakis (3,6-diphenylcarbazol-9-yl)benzene (CzTPN-Ph): mCBP (red EML) (y nm)/10 wt. % 9-(3-(9H-carbazol-9-yl)-9-(4-(4,6-diphenyl-1,3,5-triazin-2-yl)phenyl)-9H-carbazol-6-yl)-9H-carbazole (3CzTRZ): 2,8-bis (diphenylphosphoryl) dibenzo-[b,d] thiophene (PPT, blue EML) (z nm)/PPT (50 nm)/LiF/Al. In this device, the T_1 level of mCBP host is 2.9 eV, which is much higher than that of blue, green and red TADF emitters, ensuring the high efficiency. Besides, PPT has a high T_1 of 3.1 eV, suggesting a good confinement of the triplet excitons. By optimizing the charge generation zone via the adjustment of different EML thickness (the total thickness is set to be x + y + z = 15 nm), the WOLED achieved a maximum EQE of over 17%, a peak PE of 34.1 lm/W with CIE coordinates of (0.30, 0.38).

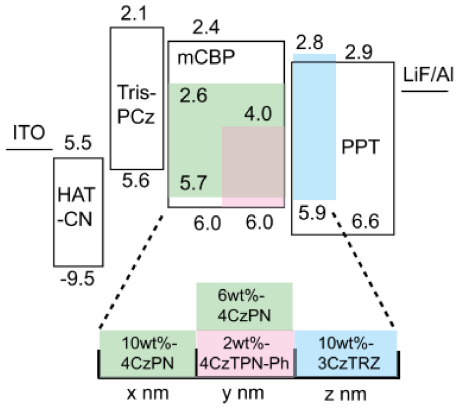

Figure 2. The WOLED structures and energy level diagram. Reproduced with permission from [55], AIP Publishing LLC, 2014.

3.2.2. WOLEDs Combining TADF Exciplex Hosts and all TADF Materials

Although TADF-based WOLEDs can exhibit high efficiency, their color-stability is still unsatisfactory. In fact, the development of TADF-based WOLED simultaneously with high efficiency, stable electroluminescent spectra and high CRI is a big challenge. Therefore, to compete with their counterparts, further improvement on emission quality is required for TADF-based WOLEDs [119–122]. To alleviate this difficulty the combination of TADF exciplex hosts and all TADF materials can be an alternative to develop WOLEDs. For this way, electron-donating and electron-accepting materials are carefully chosen to form the exciplex host, generating efficient TADF characteristic via RISC. Then, the singlet excitons on the exciplex are harvested by the TADF materials via Förster energy transfer. Besides, the two host materials should have higher T_1 than the exciplex, otherwise the triplet excitons decay non-radiatively. Moreover, the T_1 of exciplex should be higher than that of TADF emitters.

Towards this end, Zhang et al. recently constructed an efficient, color-stable and high CRI WOLED employing all TADF system, yielding a maximum forward-viewing EQE of 19.2%, PE of 46.2 lm W^{-1}, CRI of 82 and a stable color with the variation of CIE coordinates of (0.00, 0.02) at 100-3000 cd m^{-2} [123]. The optimized device configuration is ITO/4,4′-cyclohexylidenebis[*N*,*N*-bis(4-methylphenyl)aniline] (TAPC, 40 nm)/4,4′-bis(9-carbazolyl)-2,2′-dimethylbiphenyl (CDBP, 10 nm)/CDBP: 1,3,5-triazine-2,4,6-triyl)tris(benzene-3,1-diyl)tris(diphenylphosphineoxide) (PO-T2T) (2:1): 1 wt. % AnbTPA (14 nm)/CDBP:PO-T2T (3:1, 6 nm)/CDBP:PO-T2T (1.5:1): 10 wt. % 2CzPN (10 nm)/PO-T2T (45 nm)/LiF (1 nm)/Al (100 nm), where (2CzPN (1,2-bis(carbazol-9-yl)-4,5-dicyanobenzene) and AnbTPA (2,6-bis[4-(diphencylamino)phenyl]-9,10-anthracenedione) are light-blue and red TADF emitters, respectively. The high performance can be explained as follows. (i) CDBP:PO-T2T exciplex system possessing efficient TADF characteristic has been used as the host, which is beneficial to the up-conversion of triplet excitons, improving the efficiency; (ii) CDBP:PO-T2T exciplex system having suitable energy levels. For example, the HOMO of dopants are lower than that of CDBP, which can not only help the formation of the "barrier-free" structure but also minimize the trapping effects on dopants; (iii) Beneficial from the good hole and electron transporting properties from CDBP and PO-T2T respectively, the transporting ability of each EML can be precisely adjusted and balanced by controlling the ratio between CDBP and PO-T2T; (iv) An interlayer is introduced between emitting layers (EMLs) to confine the exciton, further improving the color-stability, as shown in Figure 3. This is because the 6 nm interlayer CDBP:PO-T2T can effectively prevent the energy transfer between two emitters for the Förster radius is ~3 nm, confining excitons in each EML. With precisely controlled ratios of each EML, the hole and electron transport can be balanced and excitons can be generated in the whole EML and it keeps the same exciton distributions of two EMLs under different driving voltages. Therefore, a stable color is obtained.

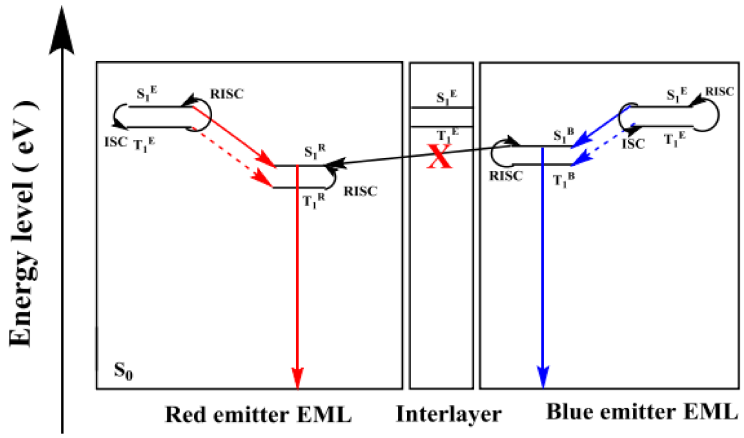

Figure 3. The exciplex host exciton energy diagram and possible decay ways of singlet and triplet excitons. (Solid arrow represents Förster energy transfer, dash arrow represents Dexter energy transfer and blocking mark represents singlet excitons energy stopping transfer). Reproduced with permission from [123], Elsevier, 2017.

3.3. WOLEDs Based on TADF and Conventional Fluorescence

3.3.1. WOLEDs Using Blue TADF and Complementary Fluorescence Materials

Given that (i) TADF materials can harvest triplet excitons; (ii) hybrid WOLEDs composed of blue fluorescence and green-red phosphorescence emitters can realize high performance [60–66], WOLEDs based on a TADF blue exciton generation combined with green and red fluorescence emitters are expected to realize the IQE of 100%. This way is inspired by the TADF-assisted fluorescence monochromatic OLEDs, where direct charge recombination on the conventional fluorescent molecules should be eliminated to obtain high IQE by using a suitable combination of TADF and fluorescent

molecules [124,125]. In other words, a TADF molecule acts as a triplet harvester for other-color fluorescent emitters to achieve white emission.

In 2015, Higuchi et al. demonstrated this approach by using blue TADF emitter bis[4-(9,9-dimethyl-9,10-dihydroacridine)phenyl]sulfone (DMACDPS) with green fluorescent emitter 9,10-bis[*N*,*N*-di-(p-tolyl)-amino]anthracene (TTPA) and red emitter tetraphenyldibenzoperiflanthene (DBP), achieving a maximum EQE of 12% [126]. The device structure is ITO/*N*,*N*′-di(naphthalen-1-yl)-*N*,*N*′-diphenyl-benzidine (α-NPD, 30 nm)/1 wt. % DBP: 10 wt. % TTPA: 1,3-bis(9-carbazolyl) benzene (mCP, 8 nm)/mCP (2 nm)/DMACDPS (7.5 nm)/bis[2-(diphenylphosphino)phenyl]ether oxide (DPEPO, 10 nm)/2,2′,2′′-(1,3,5-benzinetriyl)-tris(1-phenyl-1-H-benzimidazole) (TPBi, 40 nm)/LiF (0.5 nm)/Al (100 nm). The high performance can be explained as follows. (i) There is a large spectral overlap between the ground state absorption of the exciton acceptor and fluorescent emission of the exciton donor, indicating that the energy of singlet excitons, i.e., Förster energy transfer, up-converted from a triplet state on a TADF molecule can be efficiently transferred to the fluorescent exciton acceptors; (ii) A large LUMO energy barrier is presented at the mCP/DMACDPS interface, leading to the carrier recombination mainly occurring on DMACDPS molecules for blue emission; (iii) 2 nm spacer mCP is used to eliminate the direct carrier recombination on fluorescent molecules and produce delayed emission from the fluorescent molecules. As a consequence, the exciton donor and acceptor molecules are separated into different layers, because Förster energy transfer involves long-range interactions; (iv) The cascade energy transfer occurs from S_1 of DMACDPS to S_1 of DBP through S_1 of TTPA, in which controlling the TTPA concentration can tune the spectrum by influencing the amount of energy absorbed from DMACDPS and the rate of Förster energy transfer to DBP, as shown in Figure 4.

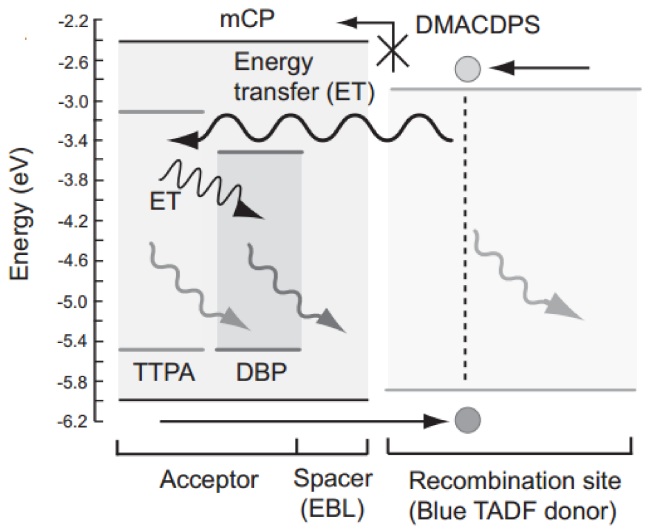

Figure 4. Schematic illustrations of a conceptual energy transfer mechanism from DMACDPS (common blue TADF emitter) to TTPA and DBP under electrical excitation. Reproduced with permission from [126], John Wiley and Sons, 2015.

3.3.2. WOLEDs Employing Yellow TADF and Complementary Fluorescence Materials

Aside from the use of above-mentioned blue TADF emitter system, the utilization of other-color TADF emitters combined the complementary fluorescence materials is also an effective way to organize WOLEDs. In principle, the TADF molecule also acts as a triplet harvester for fluorescent emitters, ensuring the high efficiency.

For example, Li et al. reported high-efficiency and high CRI WOLEDs with the chromaticity-adjustable yellow TADF emitter 2-(4-phenoxazinephenyl) thianthrene-9,9′, 10,10′-tetraoxide (PXZDSO2) [56]. By combining the conventional deep-blue fluorescence emitter NI-1-PhTPA

and PXZDSO2, the two-color WOLED showed a maximum EQE of 15.8% (device W3). Then, since the chromaticity of the EML containing PXZDSO2 could be tuned to yellowish green, they introduced a deep-red-fluorescence emitter DBP (dibenzo{[f,f′]-4,4′,7,7′-tetraphenyl}diindeno [1,2,3-cd:1′,2′,3′-lm]perylene) subtly to fabricate three-color WOLED, achieving the most efficient ever EQE of 19.2% with CRI of 68 (device W4) and the highest ever CRI of 95 with EQE of 15.6% (device W6). The configurations are ITO/hexaazatriphenylene hexacarbonitrile (HATCN)/TAPC/EMLs/TmPyPB/LiF/Al, in which device W3 has the EML of CBP: 8 wt. % NI-1-PhTPA (10 nm)/CBP (3 nm)/CBP: 6 wt. % PXZDSO2 (15 nm)/CBP (3 nm)/CBP: 8 wt. % NI-1-PhTPA (10 nm), device W4 has the EML of CBP: 7 wt. % NI-1-PhTPA (10 nm)/CBP (3 nm)/CBP: 3 wt. % PXZDSO2 (5 nm)/CBP: 5 wt. % PXZDSO2: 0.3 wt. % DBP (5 nm)/CBP: 3 wt. % PXZDSO2 (5 nm)/CBP (3 nm)/CBP: 7 wt. % NI-1-PhTPA (10 nm), device W6 has the EML of CBP: 10 wt. % NI-1-PhTPA (10 nm)/CBP (3 nm)/CBP: 5 wt.% PXZDSO2: 0.35 wt. % DBP (15 nm)/CBP (3 nm)/CBP: 10 wt. % NI-1-PhTPA (10 nm). The device working mechanisms can be described as follows. For device W3, (i) since NI-1-PhTPA is a deep-blue-fluorescence emitter and CBP: 6 wt. % PXZDSO2 emit yellow light with broad spectrum, high-performance two-color WOLEDs were realized; (ii) given the almost equal T_1 level of NI-1-PhTPA and PXZDSO2, the efficiency roll-off occurs if they are directly contact due to the triplet exciton quenching by NI-1-PhTPA; (iii) the efficiency roll-off can be further induced as the formed triplet excitons of NI-1-PhTPA cannot be utilized by PXZDSO2; (iv) to stabilize the recombination zone which occurs in whole EMLs since NI-1-PhTPA/CBP are bipolar and avoid triplet exciton quenching by NI-1-PhTPA, two 3 nm CBP were inserted between the blue and yellow EMLs, restraining the inevitable Förster energy transfer from NI-1-PhTPA to PXZDSO2; (v) to reduce the triplet exciton energy loss via nonradiative transition process, blue-fluorescence emitter was dispersed in CBP for blue emission, leading to most excitons being generated at CBP; (vi) triplet energy transferred from CBP gives most of triplet excitons of PXZDSO2 since triplet excitons typically have long diffusion lengths (≈100 nm), as shown in Figure 5a. Hence, an EQE of 15.8% was achieved for device W3. For device W4, (i) a deep-red-fluorescence emitter DBP was conceived to be used; (ii) PXZDSO2 was an assistant host for DBP to realize red light emission due to efficient energy transfer from the S_1 of PXZDSO2; (iii) the doping concentration of PXZDSO2 was decreased to reduce intermolecular aggregation and thus blue shifted emission (20 nm), achieving green emission, complementary to emissions of NI-1-PhTPA and DBP; (iv) a red EML of CBP: 5 wt. % PXZDSO2: 0.3 wt. % DBP was inserted between two green EMLs of CBP: 3 wt. % PXZDSO2 to receive singlet exciton energy transferred from the PXZDSO2 molecules in both sides to give both green and red emissions; (v) the two doped blue EMLs and CBP interlayers located at the both sides of the green EMLs to give blue emission and to confine the PXZDSO2 triplet excitons, respectively, as shown in Figure 5b. Thus, an EQE of 19.2% was achieved for device W4. Furthermore, an EML consisting of improved DBP doping concentration was utilized instead of the green and red EMLs for candle-style warm WOLEDs (device W6), achieving the high CRI of 95.

3.3.3. Single-EML WOLEDs Utilizing Blue TADF Host and Complementary Fluorescence Dopant

According to the number of EMLs, the device architectures can be simply classified into two kinds, namely multi-EML and single-EML WOLEDs [127–132]. Compared with multi-EML WOLEDs, the structures, fabrication procedures and device engineering of single-EML WOLEDs are relatively simple. For single-EML WOLEDs, by managing the incomplete energy transfer from hosts to guests in EMLs, the host materials can also be functioned as the blue emitters to produce blue emissions, in which the concentration of guests is usually low (e.g., <1%) to ensure the white emissions [133–135]. Generally, this simple single-EML structures can be used to develop any type of WOLEDs. Therefore, by carefully manipulating the charges and excitons distribution, the development of single-EML WOLEDs based on TADF is possible.

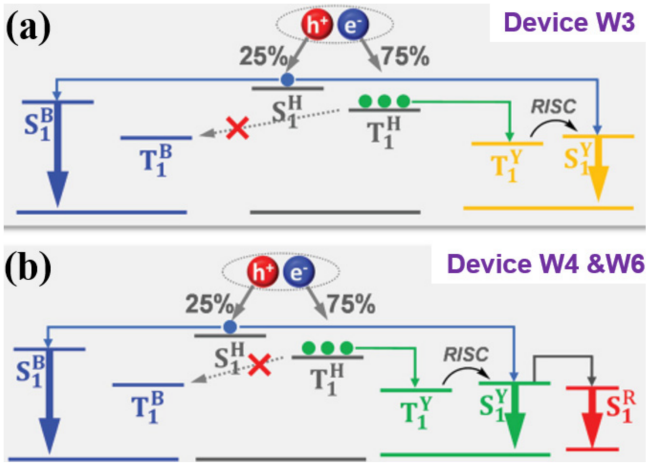

Figure 5. Device function mechanisms of the conceptual utilization of singlet and triplet excitons generated in EMLs. (**a**) device W3; and (**b**) devices W4 and W6. H, B, Y and R are CBP, NI-1-PhTPA, PXZDSO2 and DBP, respectively. Reproduced with permission from [56], John Wiley and Sons, 2016.

Zhao et al. demonstrated a single-EML WOLED by using blue host TADF material of DMAC-DPS and traditional orange fluorescent dopant of (5,6,11,12)-tetraphenyl-naphthacene (rubrene), achieving a highly efficient and color stable single-EML WOLEDs with the EQE of 7.48% and PE of 15.9 lm W^{-1} [136]. The device architecture is ITO/MoO_3 (3 nm)/4,4′,4″-tri(N-carbazolyl)triphenylamine (TCTA, 20 nm)/DMAC-DPS: 0.6 wt. % rubrene (15 nm)/4,7-diphenyl-1,10-phenanthroline (Bphen, 40 nm)/LiF (1 nm)/Al. In this single-EML WOLED, DMAC-DPS is a highly efficient blue TADF material with small ΔE_{ST} of 0.08 eV. Hence, the 75% triplets produced on this TADF host could up-convert to its S_1, then the total singlets of >25% would transfer to S_1 of dopant by Förster energy transfer process, as shown in Figure 6. Besides, the Dexter energy transfer between T_1 of host and dopant could be suppressed effectively by decreasing the doped concentration (e.g., 0.6%). Therefore, the white emission is derived from both the emissions of host and dopant through an incomplete energy transfer from the blue TADF host to orange fluorescent dopant. When a traditional fluorescent 4,4′-bis(9-ethyl-3-carbazo-vinylene)-1,1′-biphenyl (BCzVBi) is used as the host, only a maximum EQE of 3.72% can be obtained, indicating the advantage of the TADF materials in this type of WOLEDs.

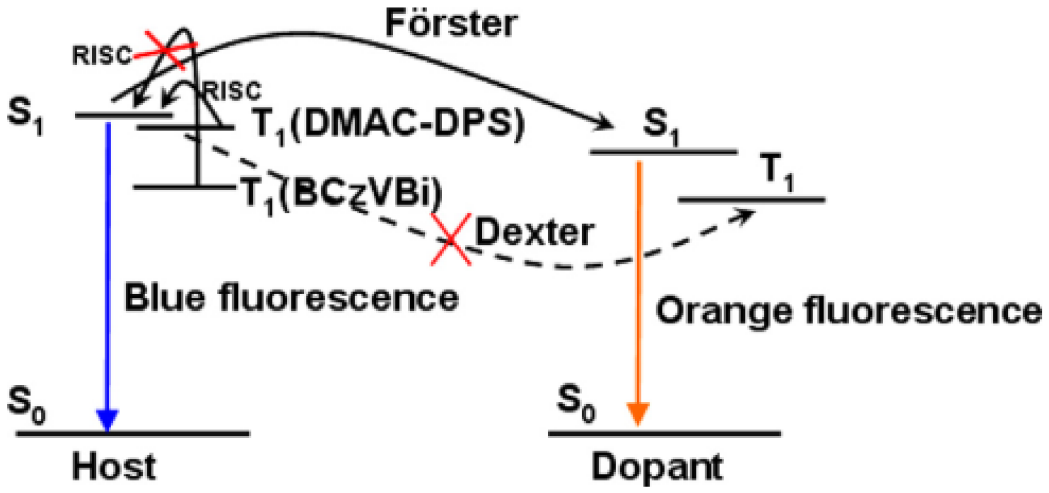

Figure 6. The energy transfer and electroluminescent emission processes in the single-EML WOLEDs based on TADF host materials. Reproduced with permission from [136], Elsevier, 2015.

3.3.4. Single-EML WOLEDs Exploiting Fluorescent Host, Blue TADF and Complementary Fluorescence Dopants

Another way to develop single-EML WOLEDs based on TADF is the exploitation of fluorescent host, blue TADF and complementary fluorescence dopants. In such way, an efficient blue TADF materials is required. Besides, the concentration of complementary fluorescence dopants should be very low, otherwise the triplet excitons could be quenched by the conventional fluorescence dopants.

In 2015, Song et al. reported this way by codoping a blue TADF emitter and a yellow fluorescence emitter into a fluorescent host, obtaining a maximum EQE of 15.5% and PE of 39.3 lm W^{-1} [137]. The device configuration is ITO (120 nm)/poly(3,4-ethylenedioxythiophene):poly(styrenesulfonate) (PEDOT:PSS, 60 nm)/TAPC (10 nm)/TCTA (10 nm)/mCP (10 nm)/DPEPO:DMAC-DPS: 2,8-ditert-butyl-5,11-bis(4-tert-butylphenyl)-6,12-diphenyltetracene (TBRb, 25 nm)/diphenylphosphine oxide-4-(triphenylsilyl)phenyl (TSPO1, 5 nm)/TPBI (30 nm)/LiF (1 nm)/Al (200 nm). The high performance can be explained as follows. (i) High-efficiency blue emitter is used, because the dominant emission mechanism is energy transfer from a blue emitter to a yellow emitter. When the concentration of DMAC-DPS is 50% in the DPEPO: DMAC-DPS blue TADF system, a maximum EQE of 22.6% can be obtained; (ii) A very low concentration of TBRb is employed (0.05%), which can not only minimize the charge trapping by TBRb but also ensure that the yellow emission induced only by Förster energy transfer process from DMAC-DPS to TBRb, as shown in Figure 7.

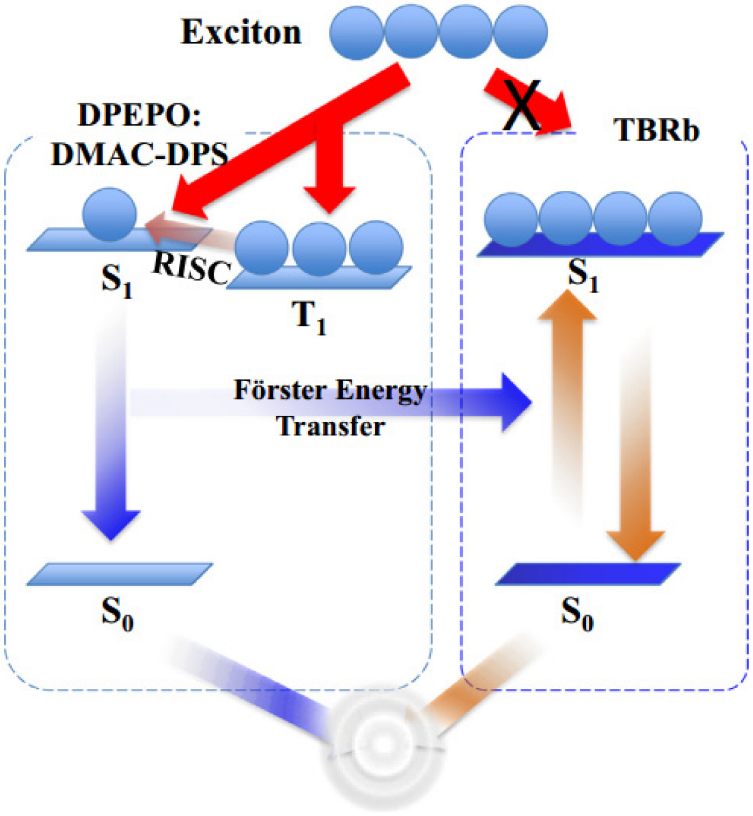

Figure 7. Schematic diagram showing the energy transfer process for maximum quantum efficiency. Reproduced with permission from [137], Elsevier, 2015.

3.3.5. Single-EML WOLEDs Comprising TADF Host and Fluorescence Dopants

Due to the simplified characteristic, another solution to realize single-EML WOLED is the use of TADF host and fluorescence dopants. For this solution, the white emission is originated from the fluorescence dopants, while the TADF host mainly functions as a triplet harvester. Besides,

the concentration of both the blue and complementary color fluorescence dopants is very low, which can reduce the charge trapping and Dexter energy transfer by the fluorescent dopants.

Song et al. described this approach by codoping a blue fluorescence emitter and a yellow fluorescence emitter into a TADF host, obtaining a maximum EQE of 14.0% and PE of 36.2 lm W^{-1} [138]. To develop the high-efficiency WOLED, they first explore a blue OLED with the structure of ITO (120 nm)/PEDOT:PSS (60 nm)/mCP (30 nm)/10-(4-((4-(9H-carbazol-9-yl)phenyl)sulfonyl)-phenyl)-9,9-dimethyl-9,10-dihydroacridine (CzAcSF): 0.3% 2,5,8,11-tetra-tert-butylperylene (TBPe) (25 nm)/TSPO1 (5 nm)/TPBI (30 nm)/LiF (1 nm)/Al (200 nm), achieving a maximum EQE of 15.4%. For this blue OLED, ~100% IQE can be realized assuming that all triplet excitons are harvested by the RISC process, as shown in Figure 8. In this blue system, efficient Förster energy can transfer from CzAcSF to TBPe, while little charge trapping by TBPe and little Dexter energy transfers from CzAcSF to TBPe due to the very low concentration of 0.3% TBPe. After the demonstration of the blue device, a single-EML WOLED has been developed. The architecture of the WOLED comprises the EML of CzAcSF: 0.3% TBPe: 0.4% 2,8-ditertbutyl-5,11-bis(4-tert-butylphenyl)-6,12-diphenyltetracene (TBRb, 25 nm), while other layers are same as those of the blue OLED. By using a low concentration of TBRb (0.4%), a pure white color of (0.31, 0.37) is obtained.

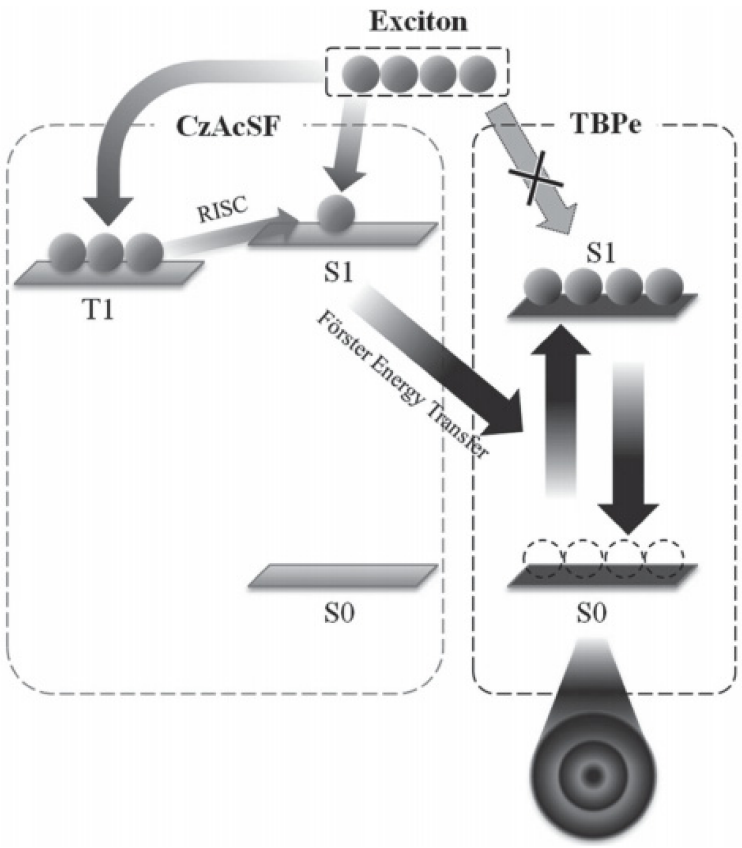

Figure 8. Schematic diagram showing the emission process of blue fluorescent device with a blue fluorescent emitter doped in a TADF host. Reproduced with permission from [138], John Wiley and Sons, 2015.

3.4. Hybrid WOLEDs Based on Blue TADF and Phosphorescence

3.4.1. Hybrid WOLEDs including Blue TADF Materials and Complementary Phosphorescence Materials

Since both TADF and phosphorescence emitters can harvest singlet and triplet excitons, the mixture of TADF and phosphorescence emitters is a significant approach to construct WOLEDs [139–141]. By virtue

of their respective advantages, high performance can be realized. In particular, there are tremendous interest in mixing blue TADF emitters with green/red or complementary color phosphorescence emitters. This is because blue TADF materials (i) are naturally advantageous to achieve high triplet energies due to their reduced singlet-triplet splits; (ii) can possess high efficiency, (iii) can harvest the triplets [142]. For this kind of WOLED (i.e., mixing blue TADF and other-color phosphorescence emitters), it is also called hybrid WOLEDs [60–66]. Previously, hybrid WOLEDs based on conventional blue fluorescent emitters have been extensively studied, since this kind of WOLEDs can show high efficiency, stable color, low voltage and long lifetime [143–153]. By replacing the conventional blue fluorescent emitters with TADF materials, high performance can also be expected.

Zhang et al. reported the first hybrid WOLEDs by using blue TADF materials, achieving a maximum forward-viewing PE of 47.6 lm/W [142]. The device structure is ITO/HATCN (5 nm)/NPB (40 nm)/TCTA (10 nm)/mCP: 4,5-bis(carbazol-9-yl)-1,2-dicyanobenzene (2CzPN, 11 nm, blue EML)/3-(4-biphenyl)-4-phenyl-5-(4-tert-butylphenyl)-1,2,4-triazole (TAZ): 4 wt. % (acetylacetonato)bis[2-(thieno[3,2-c] yridine-4-yl)phenyl]iridium(III) (PO-01, 4 nm, orange EML)/TAZ (40 nm)/LiF (0.5 nm)/Al (150 nm), as shown in Figure 9. The factors for the high performance: (i) mCP is chosen to be the host for 2CzPN due to the wide energy gap and high T_1 of 3.0 eV, since the host of the TADF material plays an important role in determining the efficiency; (ii) 2CzPN is placed nearest to the main recombination zone, ensuring that excitons can diffuse throughout the emissive region to produce a desired color-balanced output; (iii) triplets formed on 2CzPN can be harvested by either energy transfer to the low-lying triplet states of the phosphor PO-01 (2.2 eV) or thermal upconversion to the emissive singlet states, eliminating the energy loss; (iv) the recombination zone is fixed as the voltage increases by 2CzPN due to its charge trapping ability, achieving stable white emission.

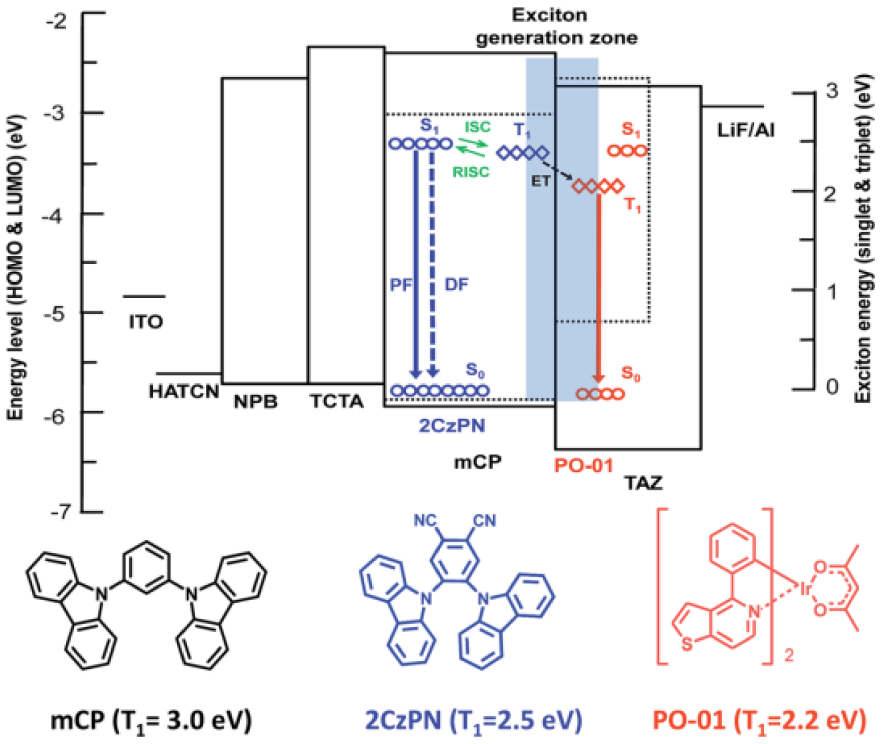

Figure 9. Schematic diagrams of the working mechanisms. The gray filled rectangle represents the main exciton generation zone. PF is the prompt fluorescence while DF is the delayed fluorescence. RISC indicates the reverse ISC and ET denotes the energy transfer. Reproduced with permission from [142], Royal Society of Chemistry, 2014.

To further enhance the performance of this type of hybrid WOLEDs, Wu et al. developed a three-color WOLED WOLEDs employing an efficient TADF material as the blue emitter, combined with red and green phosphorescent emitters, achieving the superior efficiency/CRI/color stability and low efficiency roll-off [154]. The WOLED shows the maximum EQE of 23.0%, PE of 51.7 lm W^{-1}, CRI of 89 and stable colors. The device structure is ITO (180 nm)/HATCN (10 nm)/TCTA: 20% HATCN (50 nm)/TCTA (20 nm)/mCP (10 nm)/TCTA: 8% ridium(III)bis(2,4-diphenyl-quinoline) (acetylacetonate) ($Ir(PPQ)_2(acac)$, red EML, 7 nm)/TCTA: 10% bis(2-phenylpyridine)iridium acetylacetonate ($Ir(ppy)_2(acac)$, green EML, 2.5 nm)/DPEPO: 10% DMAC-DPS (3.5 nm)/DPEPO (10 nm)/1,3-bis(3,5-dipyrid-3-yl-phenyl)benzene (BmPyPB): 3% Li_2CO_3 (35 nm)/Li_2CO_3 (1 nm)/Al (100 nm). The key strategy is the utilization of blue-green-red cascade energy transfer structure, the regulation of the doping concentration and the manipulation of charges and excitons. For the blue emission, it is originated from the TADF emitter DMAC-DPS. In the case of green emission, it is ensured by the energy transfer process between DMACDPS and $Ir(ppy)_2(acac)$. In terms of red emission, it is resulted from not only the energy transfer between $Ir(ppy)_2(acac)$ and $Ir(PPQ)_2(acac)$ but the self-charge-trapping effect, as shown in Figure 10. As a result, an efficient white emission is produced.

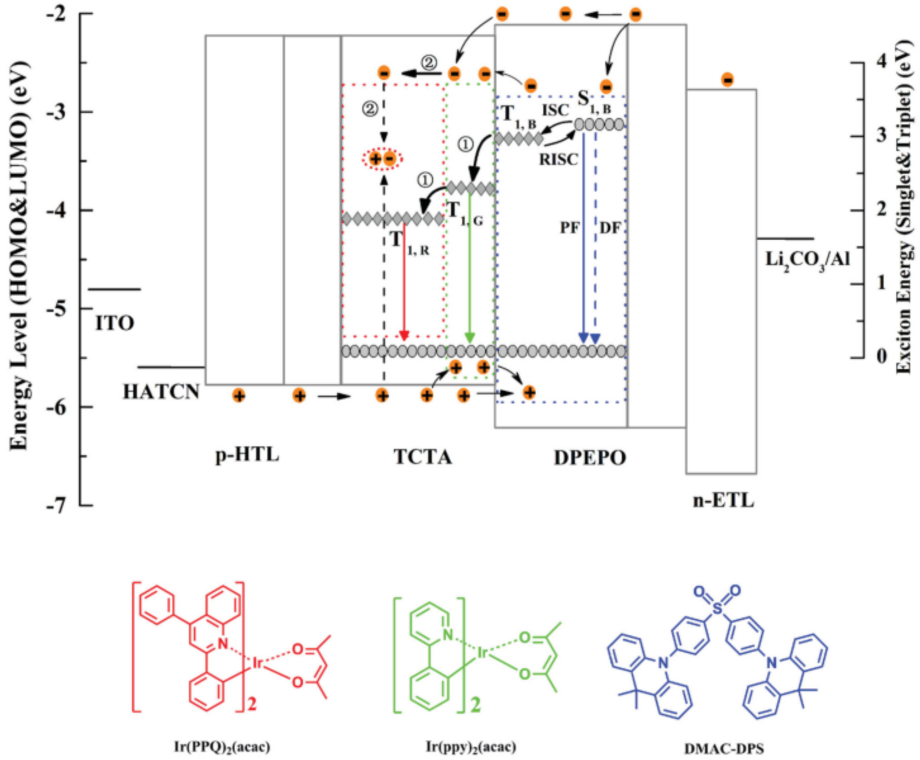

Figure 10. Proposed energy level diagram of the WOLED and chemical structures of emitters. R, G and B represent $Ir(PPQ)_2(acac)$, $Ir(ppy)_2(acac)$ and DMAC-DPS, respectively. Solid and dashed lines refer to HOMO and LUMO energy levels; circles and diamonds correspond to the exciton energies (S_0, S_1 and T_1), respectively. ① presents the energy transfer process and ② is the carrier trapping process. PF is the prompt fluorescence, DF is the delayed fluorescence. Reproduced with permission from [154], John Wiley and Sons, 2016.

Although high-performance hybrid WOLEDs based on TADF materials have been demonstrated, there are still some problems, even for these state-of-the-art devices [142,154]. For example, (i) the driving voltages are somewhat high (e.g., 3.2 V at 1 cd m^{-2} [154]); (ii) the luminances are very low (e.g., only ~10000 cd m^{-2} [154]); iii) the efficiency at high luminance is not high (e.g., <6 lm W^{-1}

at 10000 cd m^{-2} [154]); (iv) the CRI is not high enough; (v) negligible attention has been paid to the lifetime of TADF-based hybrid WOLED.

To solve the issues, Luo et al. recently reported high-performance two-color and three-color hybrid WOLEDs [155]. The two-color WOLED exhibits (i) low voltage (i.e., 2.9 V at 1 cd m^{-2}); (ii) high luminance (103756 cd m^{-2}); (iii) maximum total EQE and PE of 23.5% and 70.92 lm W^{-1}, respectively; (iv) 21.59 lm W^{-1} at 10000 cd m^{-2}. The three-color WOLED exhibits (i) low voltage and high luminance (51514 cd m^{-2}); (ii) superior CRI of 94; (iii) EQE and PE of 17.3% and 46.09 lm W^{-1}, respectively. The configuration of the two-color WOLEDs is ITO/HAT-CN (100 nm)/TAPC (20 nm)/mCP: 9,9′,9″,9‴-((6-phenyl-1,3,5-triazine-2,4-diyl)bis(benzene-5,3,1-triyl))tetrakis (9*H*-carbazole) (DDCzTrz, 10 nm, 20%)/interlayers (3 nm)/bis[2-(2-hydroxyphenyl)-pyridine] beryllium ($Bepp_2$): bis(2-phenyl-4,5-dimethylpyridinato)[2-(biphenyl-3-yl)pyridinato] iridium(III) ($Ir(dmppy)_2(dpp)$, 15 nm, 1:2%)/$Bepp_2$ (35 nm)/LiF (1 nm)/Al (160 nm), where interlayers are none, mCP and 2,6-bis(3-(carbazol-9-yl)phenyl)pyridine (26DCzPPy) for device W11, W12 and W13, respectively. The configuration of the two-color WOLED is ITO/HAT-CN (100 nm)/TAPC (20 nm)/mCP: DDCzTrz (10 nm, 20%)/26DCzPPy (interlayer, 3 nm)/$Bepp_2$: $Ir(dmppy)_2(dpp)$: $Ir(piq)_3$ (15 nm, 1:2%:1.3%)/$Bepp_2$ (35 nm)/LiF (1 nm)/Al (160 nm). Unlike previous TADF-based hybrid WOLEDs, the bipolar interlayer is demonstrated to enhance the performance. Particularly, it is demonstrated that the use of interlayer can enhance the lifetime (2.3 times). The working mechanism of the two-color WOLED can be described as follows, which is beneficial to comprehend the reason why the bipolar interlayer can enhance the performance. For W11, since mCP and $Bepp_2$ are p-type and n-type materials, respectively, holes and electrons are easily accumulated at the mCP/$Bepp_2$ interface, forming singlet and triplet excitons, as shown in Figure 11a. The triplets on blue EML can (i) convert into singlets via the RISC procedure and then generate the blue emission; (ii) transfer to the low-energy of yellow phosphor $Ir(dmppy)_2(dpp)$ via the Dexter process and then generate part of yellow emission (the other part of yellow emission is originated from excitons on the yellow EML). However, the main exciton generation zone of W11 is narrow, unfavorable to the performance. Similarly, the main exciton generation zone of W12 is located at the mCP interlayer/$Bepp_2$ interface, as shown in Figure 11b. As a result, excitons are more easily harvested by $Ir(dmppy)_2(dpp)$ instead of DDCzTrz since $Ir(dmppy)_2(dpp)$ is close to the main exciton generation zone. However, a part of electrons can pass through the thin interlayer via the tunneling process and then meet holes, which can generate excitons to guarantee the blue emission. For W13, by way of the bipolar interlayer and the suitable energy levels of 26DCzPPy, both holes and electrons can be easily passed through 26DCzPPy, as shown in Figure 11c. As a result, excitons can be formed at both the mCP/26DCzPPy and 26DCzPPy/$Bepp_2$ interface, leading to a broad exciton generation zone, which ensure the high performance of W23. Besides, since the Dexter energy transfer from DDCzTrz to $Ir(dmppy)_2(dpp)$ is also prevented due to the 3 nm 26DCzPPy, the yellow emission mainly results from excitons on the yellow EML.

To simplify the device architecture, single-EML WOLEDs based on blue TADF and phosphorescence have been reported. For example, Song et al. codoped a blue TADF emitter and a yellow phosphorescent emitter into a fluorescent host, achieving the WOLED with a maximum EQE of 22.4% and PE of 60.3 lm W^{-1} [156]. The device structure is ITO (120 nm)/PEDOT:PSS (60 nm)/TAPC (20 nm)/mCP (10 nm)/DPEPO: 50% DMAC-DPS: 0.3% PO-01 (25 nm)/TSPO1 (5 nm)/TPBI (30 nm)/LiF (1nm)/Al (200 nm). The emission mechanism of this single-EML WOLED can be described as follows. (i) Due to the low concentration of PO-01 (0.3%), the direct charge trapping is not the main emission process of PO-01 to generate yellow emission; (ii) The energy can be directly transferred from DPEPO to PO-01 or from the singlet and triplet excitons of DMAC-DPS to PO-01, producing the yellow emission; (iii) The energy can be transferred from the singlet excitons of DMAC-DPS generated by the RISC of the triplet excitons of DMAC-DPS to PO-01. Therefore, both the original singlet excitons and up-converted singlet excitons of DMAC-DPS transfer emission energy to PO-01 for white emission, as shown in Figure 4.

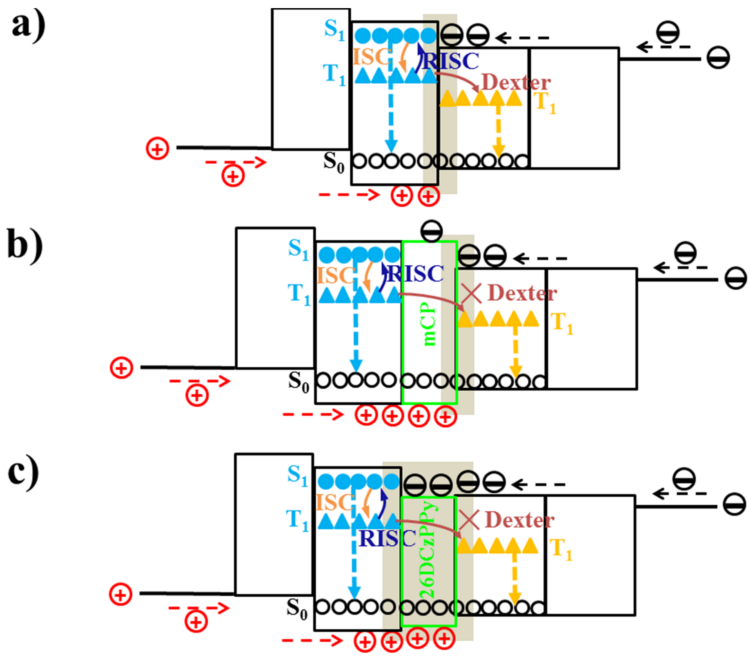

Figure 11. Schematic illustration of the working mechanism of (**a**) W11; (**b**) W12 and (**c**) W13. The gray filled rectangles are the main exciton generation zones. The Dexter energy transfer can occur in W11, while it is prohibited in both W12 and W13. Reproduced with permission from [155], Elsevier, 2017.

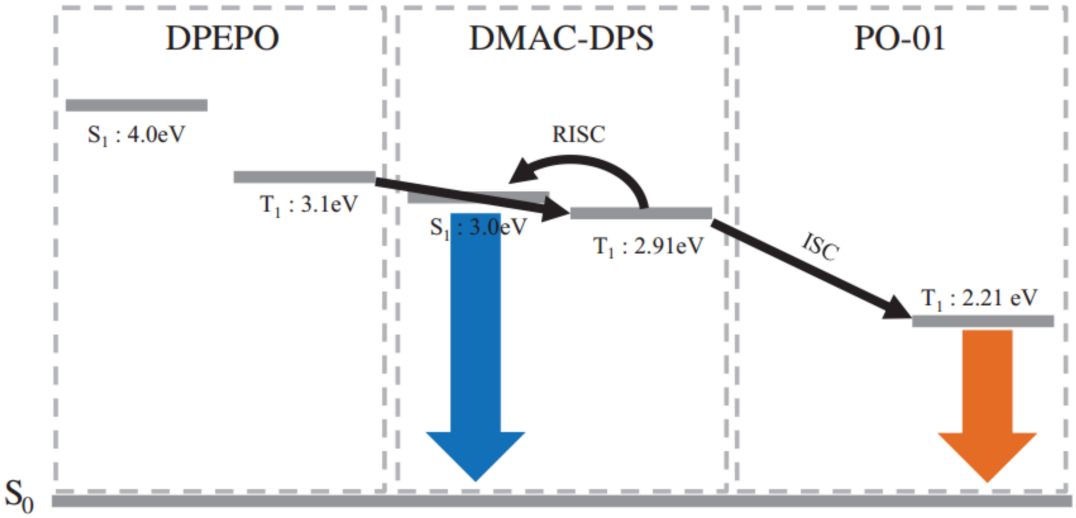

Figure 12. Schematic diagram showing the energy transfer process of the white EML. Reproduced with permission from [156], IOP Publishing, 2015.

3.4.2. Hybrid WOLEDs Possessing Blue TADF Exciplex and Complementary Phosphorescence Materials

Similar to blue TADF materials, blue TADF exciplexes, formed by mixing donor and acceptor molecules, can also be as the emitter in hybrid WOLEDs. To realize high performance, the highly efficient blue TADF exciplex system is required [157–161]. Besides, the blue exciplex system can provide a "barrier-free" architecture and a bipolar EML, which is also beneficial to the performance. To accomplish this approach, the T_1 of the blue exciplex should be higher than that of phosphorescence materials.

Liu et al. reported a single-EML hybrid WOLED by using a blue TADF exciplex CDBP: 50 wt. % PO-T2T, achieving the forward-viewing EQE of 25.5% and PE of 84.1 lm W^{-1} [162]. The device structure is ITO/TAPC (30 nm)/CDBP (10 nm)/CDBP: 50 wt. % PO-T2T: 0.1 wt. % $Ir(ppy)_2acac$: 0.3 wt. % bis(2-methyldibenzo [f,h]quinoxaline)(acetylacetonate)iridium (III) ($Ir(MDQ)_2acac$, 30 nm)/PO-T2T (40 nm)/LiF (1 nm)/Al (100 nm). The emission mechanism of this device can be explained as follows. A system with low green/red phosphorescent dopants and conventional blue fluorescent host molecules is shown in Figure 13a. In Zone I, both singlets and triplets of the blue host can transfer energy to dopants, giving theoretically 100% IQE emission from dopant. In Zone II, only triplets of the host can reach the dopant due to the different diffusion length of singlets and triplets. In this case, blue emission from the host and green/red emission from dopant can be obtained with theoretically 100% IQE. In Zone III, no exciton from the host can reach the dopant, giving only blue emission with an IQE of 25%. Therefore, 100% IQE white emission can only be achieved in Zone II but with warm-white emission, while the white balance can be maintained in Zone III but with 25% IQE. These issues can be effectively addressed by using a blue TADF host, as shown in Figure 13b. For this system, both singlet and triplet excitons in Zone III can be harvested for blue emission with a theoretical 100% IQE. Thus, a TADF host-phosphor dopant WOLED can simultaneously achieve 100% IQE and white emission even with extremely low dopant concentrations. Besides, due to the extremely small ΔE_{ST}, blue TADF emitters intrinsically have T_1s higher than those of the green phosphors.

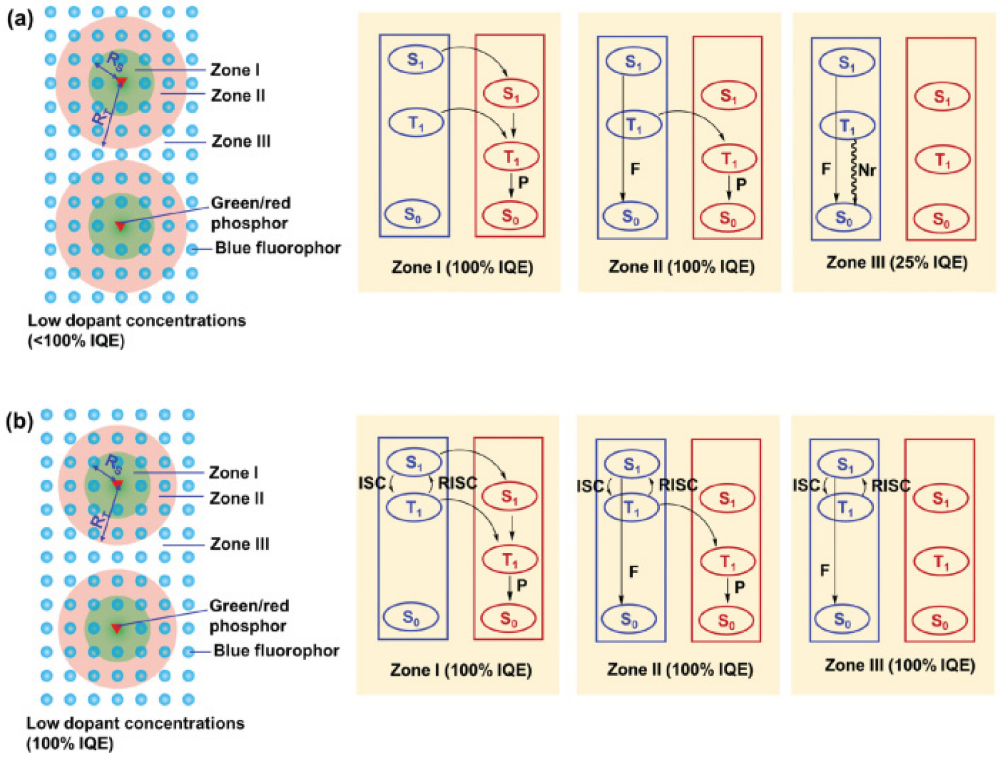

Figure 13. Schematic diagrams for management of singlet and triplet excitons in single-EML hybrid WOLEDs based on (**a**) conventional blue fluorophores and (**b**) TADF blue emitters with low dopant concentrations. Green circle coverage represents diffusion zone of singlets (Zone I). Pink circle coverage represents diffusion zone of triplets (Zone II). The uncovered zone is Zone III; for conventional blue fluorophores, all singlets and triplets formed in this zone cannot reach the phosphor molecules and only singlets can be used for emission; for TADF blue emitters, triplets can be up-converted into S_1 for emission together with the directly generated singlets. R_S and R_T are respectively diffusion lengths of singlet and triplet excitons; compared with conventional host, R_T of TADF host is smaller due to the fast competition process of RISC. F, fluorescence; P, phosphorescence; Nr, nonradiative decay. Reproduced with permission from [162], John Wiley and Sons, 2015.

To further improve the performance of hybrid WOLEDs possessing blue TADF exciplex and complementary phosphorescence materials, precise exciton allocation is significant, aside from the use of efficient blue TADF exciplex [163–165]. Particularly, the notorious efficiency roll-off problem can be solved by dint of precise exciton allocation, given that high triplet exciton density at high luminance deteriorates the efficiency [166–170].

Wu et al. recently demonstrated a series of high-performance WOLEDs, by managing the exciton allocation [171]. For example, they fabricated the all-fluorescence WOLEDs using blue TADF exciplex host and TBRb as the guest (CDBP:PO-T2T:TBRb), achieving the forward-viewing EQE of 20.8% and PE of 75.4 lm W^{-1}, the highest values for all-fluorescence WOLEDs. Then, they developed hybrid WOLEDs with low efficiency roll-off, obtaining two-color hybrid WOLEDs with maximum EQE of 28.3% and PE of 102.9 lm W^{-1}, remaining 25.8% and 63.5 lm W^{-1} at 1000 cd m^{-2}. Furthermore, a three-color WOLED yields a CRI of 86, an EQE of 29.4% and PE of 75.5 lm W^{-1}. The structure of fluorescent WOLED is ITO/MoO_3 (10 nm)/TAPC: MoO_3 (20.0%, 50 nm)/CDBP (10 nm)/CDBP:PO-T2T:TBRb (1:1, 0.3%, 20 nm)/PO-T2T (10 nm)/PO-T2T: Li_2CO_3 (3%, 45 nm) /Li_2CO_3 (1 nm)/Al (100 nm). The tri-EML hybrid WOLED with the EML of CDBP:PO-T2T: PO-01 (4:1, 5%, 3 nm)/CDBP:PO-T2T: PO-01 (1:1, 0.3%, 8 nm)/CDBP:PO-T2T: PO-01 (1:4, 5%, 3 nm), while other layers are the same as those of fluorescent WOLED. In their devices, nearly all electrically produced singlet and triplet excitons can be efficiently utilized for white emission, yielding the unity EQE. Besides, with the help of exciplex-sandwich emissive architecture, the performance of hybrid WOLEDs are among the best WOLEDs. As shown in Figure 14, because the blue exciplex possesses high T_1, the generated triplet excitons on the blue-EML can be transferred to the adjacent green-EML and then the red-EML for radiative decay, producing the white emission. For this sandwich-EML, it not only confines singlets and triplets into the emissive zone but also utilize all singlets and triplets because the diffused excitons from the middle emissive zone can undergo radiative transition in the bilateral emissive zone. Therefore, the unity exciton utilization ratio is achieved by this unique working mechanism.

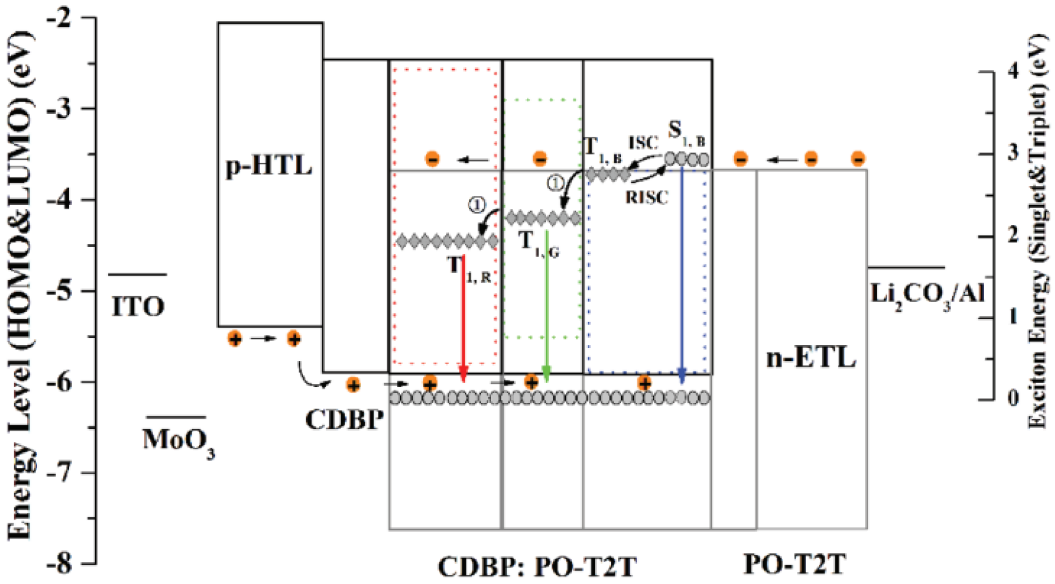

Figure 14. Schematic diagrams showing exciton allocation in the emissive zone. Reproduced with permission from [171], John Wiley and Sons, 2017.

3.5. WOLEDs Based on TADF Exciplex Host and Phosphorescence Dopants

By combining high-T_1 p-type materials and high-T_1 n-type materials, high-T_1 exciplexes can be formed. When the T_1 of exciplex is higher than that of blue phosphorescence dopant, high-performance

WOLEDs can be realized by using such high-T_1 exciplexes as the host of phosphorescence dopants. In general, TADF exciplexes are promising to meet the requirement of high T_1 [36]. Therefore, the utilization of TADF exciplex host can not only nearly eliminate the charge injection barrier issue but also give an efficient TADF upconversion due to the intermolecular donor-acceptor construction and sufficiently small S_1-T_1 splitting (<0.1 eV). Moreover, the relatively high T_1 of exciplex will reduce the energy back-transfer (i.e., from $T_{1,\,guest}$ to $T_{1,\,host}$) rate constant, preventing the exciton leakage. Hence, TADF exciplex hosts can possibly make a tradeoff among the 100% IQE, low voltage and good exciton confinement in the EML. However, in such way, it would be better that both the T_1 of donor and acceptor materials are higher than that of exciplexes, otherwise the triplets in the EML could be quenched.

Wu et al. reported a single-EML WOLED by using donor mCP and acceptor 4,6-bis[3,5-(dipyrid-4-yl)phenyl]-2-methylpyrimidine (B4PyMPM) as the TADF exciplex host of phosphorescence dopants, obtaining a maximum forward-viewing EQE of 28.1% and PE of 105.0 lm W^{-1} [36]. The configuration is ITO (110 nm)/TAPC (40 nm)/TCTA (10 nm)/mCP (10 nm)/mCP: 50 wt. % B4PyMPM: 15 wt. % bis(3,5-diuoro-2-(2-pyridyl)phenyl-(2-carboxypyridyl) iridium III (FIrpic): 0.2 wt. % PO-01 (20 nm)/B4PyMPM (50 nm)/Liq (0.8 nm)/Al (120 nm). The high performance can be explained as follows. (i) The exciplex was exclusively as the host and at the same time codoped it with two-color phosphors, prohibiting the shortcomings of low efficiency and pronounced efficiency roll-off; (ii) By using energy level matching hole and electron transporting layer, the structural heterogeneity is reduced. Besides, high hole mobility of mCP (5×10^{-4} cm^2 V^{-1} s^{-1}) and electron mobility of B4PyMPM (1×10^{-4} cm^2 V^{-1} s^{-1}) are used, realizing low voltages (e.g., 1 cd m^{-2} at 2.5 V); (iii) The perfectly confined excitons fully eliminate the exciton leakage from the emission zone, enhancing the efficacy. As shown in Figure 15 left, if acceptor molecules with low T_1, part of excitons from the exciton formation zone will be trapped by the acceptor (transfer mode I). Hence, excitons transferred to the acceptor molecules would decay via a nonradiative path owing to their rather low photoluminescence quantum yields, thereby causing undesirable exciton leakage and accordingly low efficiency. As shown in Figure 15 right, if acceptor molecules with high T_1, the leakage phenomenon is suppressed (transfer mode II). Hence, all excitons are transferred only to the emitter molecules via either long-range dipole-dipole coupling (Förster energy transfer) or short-range exchange interaction (Dexter energy transfer). Thus, the emitter molecules can utilize all excitons and consequently deliver a 100% IQE.

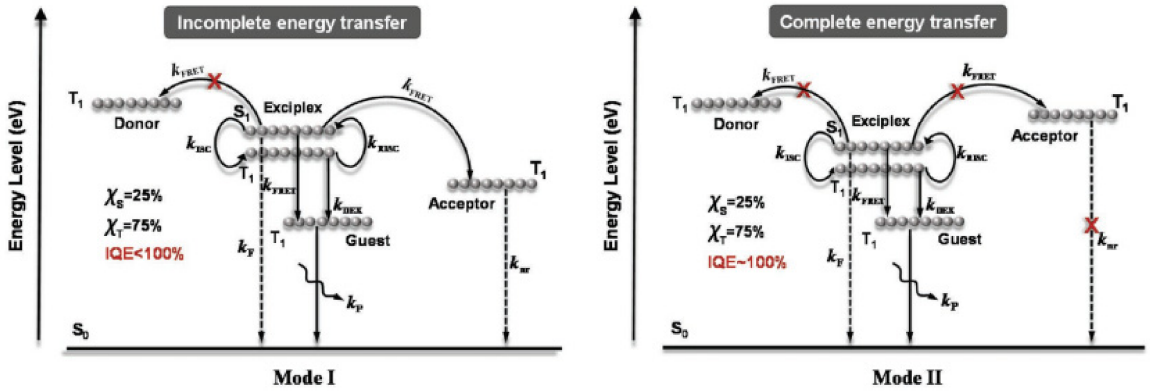

Figure 15. Two different energy-transfer modes. Donor and acceptor are the constituting molecules for exciplex. S_1 and T_1 are the singlet and triplet states, respectively. k_{FRET}, k_{DEX}, k_{ISC}, k_{RISC}, k_F and k_P are the rate constant of Förster energy transfer, Dexter energy transfer, ISC, RISC, fluorescence and phosphorescence processes, respectively. Left: Incomplete energy transfer. Right: Complete energy transfer. Reproduced with permission from [36], John Wiley and Sons, 2017.

4. Summary and Outlook

As a novel kind OLED emitter, TADF materials show many unique characteristics, which have been demonstrated to develop high-performance WOLEDs. Thanks to the hard endeavors of researchers, the performance of WOLEDs based on TADF is now comparable to state-of-the-art phosphorescence WOLEDs and hybrid WOLEDs. In this review, the focus is the development of WOLEDs based on TADF. Specifically, we highlight the recent development of WOLEDs based on all TADF emitters, WOLEDs based on TADF and conventional fluorescence emitters, WOLEDs based on TADF and phosphorescence emitters, and WOLEDs based on TADF exciplex host and phosphorescence dopants. The detailed performance of representative WOLEDs based on TADF are shown in Table 1.

Table 1. Summary of the performances of WOLEDs based on TADF.

Devices [a]	V_{on}/V_{1000} [b] (v)	EQE_{max}/EQE_{1000} [c] (%)	CE_{max}/CE_{1000} [d] (cd A^{-1})	PE_{max}/PE_{1000} [e] (lm W^{-1})	CIE_{1000} [f]	CRI [g]
Ref. [36]	2.5/3.6	28.1/21.5	83.6/61.0	105/59.5	(0.40, 0.48)	-
Ref. [55]	3.6/7.8	17/8.5	45.6/20.6	34.1/8.3	(0.33, 0.41)	-
Ref. [56]	3.4/5.4	19.2/14.2	51.4/37.3	47.5/21.8	(0.348, 0.457)	69
Ref. [123]	2.5/-	19.2/-	36.7/-	46.2/-	(0.33, 0.38)	82
Ref. [126]	-/-	12.1/-	-/-	22.0/-	(0.25, 0.31)	74
Ref. [136]	2.48/-	7.48/7.31	20.2/19.8	15.9/14.7	(0.36, 0.44)	-
Ref. [137]	-/4.3	15.5/13.3	38.4/31.9	39.3/23.4	(0.28, 0.35)	58.6
Ref. [138]	-/-	15.2/11.8	35.1/28.4	36.2/18.9	(0.31, 0.37)	-
Ref. [142]	-/-	22.5/15.4	-/-	47.6/-	(0.45, 0.48)	-
Ref. [154]	3.2/4.2	23.0/17.5	51.0/39.5	51.7/39.5	(0.438, 0.438)	89
Ref. [155]	2.9/4.65	23.5/15.1	-/-	70.92/30.09	(0.30, 0.49)	50
Ref. [156]	3.0/4.3	22.4/18.3	57.6/45.6	60.4/33.6	(0.30, 0.37)	-
Ref. [162]	2.5/-	25.5/14.8	67.0/37.0	84.1/24.2	(0.40, 0.43)	-
Ref. [171]	2.5/-	28.3/25.8	88.7/80.9	102.9/63.5	(0.46, 0.43)	86

[a] The structures are mentioned before. [b] The turn-on voltage (1 cd/m^2) and the voltage at 1000 cd/m^2. [c] Maximum EQE and the EQE at 1000 cd/m^2.[d] Maximum current efficiency (CE) and the CE at 1000 cd/m^2. [e] Maximum PE and the PE at 1000 cd/m^2. [f] CIE coordinates at about 1000 cd/m^2. [g] Maximum CRI.

Although the performance of WOLEDs based on TADF has been enhanced over the past few years, there are still many challenges before they can be large-scale commercialized production, such as the efficiency, lifetime, color-stability and cost. However, it is deserved to point out that these issues are also hindrances for other kind of WOLEDs. For the issue of efficiency, there is still much room for the efficiency of WOLEDs to the theoretical limit of 248 lm W^{-1} (standard light source (D65) from 400 to 700 nm wavelength) [172]. Generally, the EQE is decided by the photoluminescence quantum efficiency of the emissive materials (TADF or other type emitters), the fraction of excitons that can potentially radiatively decay, the charge balance and outcoupling factor, while the PE is also affected by the driving voltage. Therefore, the selection of excellent materials [173–176], the careful manipulation of charges and excitons distribution [177–180] and the introduction of outcoupling technique [181–184] are crucial helpful to the efficiency. In addition, the introduction of tandem architecture is beneficial to the efficiency [185–189]. Besides, despite high-efficiency WOLEDs based on TADF can be realized, most of the reported works suffer from the serious efficiency roll-off, particularly for the PE roll-off. As a consequence, only low efficiency can be attained at high luminances, which is not beneficial to the practical applications. To loosen this bottleneck, the charge balance, energy barriers between nearby layers and materials selection should be well manipulated [190–193].

For the lifetime, no long-lifetime WOLEDs based on TADF has been reported so far, indicating that WOLEDs based on TADF still lag behind other kinds of WOLEDs. For example, fluorescence WOLEDs can show a long lifetime of 150,000 h at an initial luminance of 1000 cd m^{-2} [194], while hybrid WOLEDs based on conventional blue fluorescence emitters can possess a long lifetime of >30,000 h at 1000 cd/m^2 [153]. Hence, to alleviate this difficulty, stable TADF emitters are needed to be urgently explored. Another issue for WOLEDs based on TADF required to be instantly enhanced is the color-stability, since stale color is significant to the lighting and displays [195–199]. However, no WOLED based on TADF has been reported to show extremely stable color [ΔCIE = (0.00, 0.00)] in the whole luminance/driving voltage. Considering that fluorescence WOLEDs, hybrid WOLEDs based on conventional blue fluorescence emitters or even phosphorescence WOLEDs can exhibit extremely stable color [26,39], this gap between WOLEDs based on TADF and other kind of WOLEDs is very urgent to narrow (e.g., by harnessing charges and excitons distribution [39]).

In the case of the cost issue, TADF emitters are promising to lower the cost, since they naturally possess the noble metal-free characteristics. Besides, simple fabrication techniques (e.g., solution-processed technology [200–203]) and simplified device structures (e.g., doping-free architectures [204–207]) are conducive. By virtue of these technologies, the cost of WOLEDs based on TADF can be further reduced. Moreover, it is deserved to consider the innovation of excellent yet cheap materials [208–210], which is also beneficial to reduce the cost. By overcoming these obstructions, the mass production of WOLEDs may be expected.

Acknowledgments: The authors are grateful to the financial support from Scientific Research Starting Foundation of Foshan University (Gg040926, 040973), the National Natural Science Foundation of China (Grant No. 61575041, 61704034), Foshan Science and technology innovation special funds (Grant No. 2017EZ100111) and the Key Platforms and Research Projects of Department of Education of Guangdong Province (Grant No. 2016KTSCX034).

Author Contributions: Peng Xiao, Jianing Xie, Dongxiang Luo and Baiquan Liu conceived the idea; Peng Xiao, Ting Dong and Baiquan Liu wrote the paper, Jianing Xie, Dongxiang Luo, Jian Yuan and Baiquan Liu advised the paper. All authors reviewed the paper.

Conflicts of Interest: The authors declare no conflict of interest.

References

1. Camara, C.G.; Escobar, J.V.; Hird, J.R.; Putterman, S.J. Correlation between nanosecond X-ray flashes and stick-slip friction in peeling tape. *Nature* **2008**, *455*, 1089–1092. [CrossRef]
2. Ducrot, E.; Chen, Y.; Bulters, M.; Sijbesma, R.P.; Creton, C. Toughening elastomers with sacrificial bonds and watching them break. *Science* **2014**, *344*, 186–189. [CrossRef] [PubMed]

3. Boldyreva, E. Mechanochemistry of inorganic and organic systems: What is similar, what is different? *Chem. Soc. Rev.* **2013**, *42*, 7719–7738. [CrossRef] [PubMed]
4. Wang, X.; Xu, C.-N.; Yamada, H.; Nishikubo, K.; Zheng, X.-G. Electro-Mechano-Optical Conversions in Pr^{3+}-Doped $BaTiO_3$-$CaTiO_3$ Ceramics. *Adv. Mater.* **2005**, *17*, 1254–1258. [CrossRef]
5. Yu, J.H.; Kwon, S.-H.; Petrášek, Z.; Park, O.K.; Jun, S.W.; Shin, K.; Choi, M.; Il Park, Y.; Park, K.; Na, H.B.; et al. High-resolution three-photon biomedical imaging using doped ZnS nanocrystals. *Nat. Mater.* **2013**, *12*, 359–366. [CrossRef] [PubMed]
6. Wei, X.Y.; Wang, X.; Kuang, S.Y.; Su, L.; Li, H.Y.; Wang, Y.; Pan, C.; Wang, Z.L.; Zhu, G. Dynamic Triboelectrification-Induced Electroluminescence and its Use in Visualized Sensing. *Adv. Mater.* **2016**, *28*, 6656–6664. [CrossRef] [PubMed]
7. Bernanose, A.; Comte, M.; Vouaux, P. A new method of emission of light by certainorganic compounds. *J. Chim. Phys.* **1953**, *50*, 64–68. [CrossRef]
8. Pope, M.; Kallmann, H.P.; Magnante, P. Electroluminescence in organic crystals. *J. Chem. Phys.* **1963**, *38*, 2042–2043. [CrossRef]
9. Tang, C.W.; VanSlyke, V.A. Organic Electroluminescent Diodes. *Appl. Phys. Lett.* **1987**, *51*, 913. [CrossRef]
10. Yang, X.; Zhou, G.; Wong, W.-Y. Functionalization of Phosphorescent Emitters and Their Host Materials by Main-Group Elements for Phosphorescent Organic Light-Emitting Devices. *Chem. Soc. Rev.* **2015**, *44*, 8484–8575. [CrossRef] [PubMed]
11. Tyan, Y.S. Organic Light-Emitting-Diode Lighting Overview. *J. Photonics Energy* **2011**, *1*, 011009. [CrossRef]
12. Liu, B.; Gao, D.; Wang, J.; Wang, X.; Wang, L.; Zou, J.; Ning, H.; Peng, J. Progress of White Organic Light-Emitting Diodes. *Acta Phys. Chim. Sin.* **2015**, *31*, 1823–1852.
13. Burroughes, J.H.; Bradley, D.D.C.; Brown, A.R.; Marks, R.N.; Mackay, K.; Friend, R.H.; Burns, P.L.; Homes, A.B. Light-Emitting Diodes Based on Conjugated Polymers. *Nature* **1990**, *347*, 539. [CrossRef]
14. Sun, Q.J.; Wang, Y.A.; Li, L.S.; Wang, D.; Zhu, T.; Xu, J.; Yang, C.; Li, Y. Bright, Multicoloured Light-emitting Diodes Based on Quantum Dots. *Nat. Photonics* **2007**, *1*, 717–722. [CrossRef]
15. Dai, X.L.; Zhang, Z.X.; Jin, Y.Z.; Niu, Y.; Cao, H.J.; Liang, X.Y.; Chen, L.W.; Wang, J.P.; Peng, X.G. Solution-Processed, High Performance Light-Emitting Diodes Based on Quantum Dots. *Nature* **2014**, *515*, 96–100. [CrossRef] [PubMed]
16. Chen, Z.; Nadal, B.; Mahler, B.; Aubin, H.; Dubertret, B. Quasi-2D Colloidal Semiconductor Nanoplatelets for Narrow Electroluminescence. *Adv. Funct. Mater.* **2014**, *24*, 295–302. [CrossRef]
17. Li, J.; Xu, L.; Wang, T.; Song, J.; Chen, J.; Xue, J.; Dong, Y.; Cai, B.; Shan, Q.; Han, B.; et al. 50-Fold EQE Improvement up to 6.27% of Solution-Processed All-Inorganic Perovskite $CsPbBr_3$ QLEDs via Surface Ligand Density Control. *Adv. Mater.* **2017**, *29*, 1603885. [CrossRef] [PubMed]
18. Ji, W.; Liu, S.; Zhang, H.; Wang, R.; Xie, W.; Zhang, H. Ultrasonic Spray Processed, Highly Efficient All-Inorganic Quantum-Dot Light-Emitting Diodes. *ACS Photonics* **2017**, *4*, 1271–1278. [CrossRef]
19. Jiang, C.; Liu, H.; Liu, B.; Zhong, Z.; Zou, J.; Wang, J.; Wang, L.; Peng, J.; Cao, Y. Improved performance of inverted quantum dots light emitting devices by introducing double hole transport layers. *Org. Electron.* **2016**, *31*, 82–89. [CrossRef]
20. He, Z.; Zhong, C.; Su, S.; Xu, M.; Wu, H.; Cao, Y. Enhanced power-conversion efficiency in polymer solar cells using an inverted device structure. *Nat. Photonics* **2012**, *6*, 591–595. [CrossRef]
21. Jeong, J.; Seo, J.; Nam, S.; Han, H.; Kim, H.; Anthopoulos, T.D.; Bradley, D.D.C.; Kim, Y. Significant stability enhancement in high-efficiency polymer: Fullerene bulk heterojunction solar cells by blocking ultraviolet photons from solar light. *Adv. Sci.* **2016**, *3*, 1500269. [CrossRef] [PubMed]
22. Zhu, L.; Wang, L.; Xue, F.; Chen, L.; Fu, J.; Feng, X.; Li, T.; Wang, Z.L. Piezo-phototronic effect enhanced flexible solar cells based on n-ZnO/p-SnS core-shell nanowire array. *Adv. Sci.* **2016**, *4*, 1600185. [CrossRef] [PubMed]
23. Xiao, Z.; Liu, F.; Geng, X.; Zhang, J.; Ding, L. A carbon-oxygen-bridged ladder-type building block for efficient donor and acceptor materials used in organic solar cells. *Sci. Bull.* **2017**, *62*, 1331–1336. [CrossRef]
24. Yang, X.; Zhou, G.; Wong, W.-Y. Recent Design Tactics for High Performance White Polymer Light-Emitting Diodes. *J. Mater. Chem. C* **2014**, *2*, 1760–1778. [CrossRef]
25. Jou, J.-H.; Kumar, S.; Agrawal, A.; Li, T.-H.; Sahoo, S. Approaches for Fabricating High Efficiency Organic Light Emitting Diodes. *J. Mater. Chem. C* **2015**, *3*, 2974–3002. [CrossRef]

26. Liu, B.; Li, X.; Tao, H.; Zou, J.; Xu, M.; Wang, L.; Peng, J.; Cao, Y. Manipulation of Exciton Distribution for High-Performance Fluorescent/Phosphorescent Hybrid White Organic Light-Emitting Diodes. *J. Mater. Chem. C* **2017**, *5*, 7668–7683. [CrossRef]
27. Sasabe, H.; Kido, J. Development of High Performance OLEDs for General Lighting. *J. Mater. Chem. C* **2013**, *1*, 1699–1707. [CrossRef]
28. Wang, Q.; Ma, D. Management of Charges and Excitons for High-performance White Organic Light-emitting Diodes. *Chem. Soc. Rev.* **2010**, *39*, 2387–2398. [CrossRef] [PubMed]
29. Kamtekar, K.T.; Monkman, A.P.; Bryce, M.R. Recent Advances in White Organic Light-Emitting Materials and Devices (WOLEDs). *Adv. Mater.* **2010**, *22*, 572–582. [CrossRef] [PubMed]
30. Gather, M.C.; Kohenen, A.; Meerholz, K. White Organic Light-Emitting Diodes. *Adv. Mater.* **2011**, *23*, 233–248. [CrossRef] [PubMed]
31. Kido, J.; Hongawa, K.; Okuyama, K.; Nagai, K. White Light-Emitting Organic Electroluminescent Devices Using the Poly (*N*-vinylcarbazole) Emitter Layer Doped with Three Fluorescent Dyes. *Appl. Phys. Lett.* **1994**, *64*, 815. [CrossRef]
32. Kido, J.; Kimura, M.; Nagai, K. Multilayer White Light-Emitting Organic Electroluminescent Device. *Science* **1995**, *267*, 1332–1334. [CrossRef] [PubMed]
33. Yamae, K.; Kittichungchit, V.; Ide, N.; Ota, M.; Komoda, T. Invited Paper: Highly Efficient White OLEDs with Over 100 lm/W for General Lighting. In *SID Symposium Digest of Technical Papers*; Blackwell Publishing Ltd.: Hoboken, NJ, USA, 2014; p. 682.
34. Ou, Q.D.; Zhou, L.; Li, Y.Q.; Chen, S.; Chen, J.D.; Li, C.; Wang, Q.K.; Lee, S.T.; Tang, J.X. Light-Emitting Diodes: Extremely Efficient White Organic Light-Emitting Diodes for General Lighting. *Adv. Funct. Mater.* **2014**, *24*, 7249. [CrossRef]
35. Liu, B.; Wang, L.; Xu, M.; Tao, H.; Gao, D.; Zou, J.; Lan, L.; Ning, H.; Peng, J.; Cao, Y. Extremely Stable-color Flexible White Organic Light-emitting Diodes with Efficiency Exceeding 100 lm W^{-1}. *J. Mater. Chem. C* **2014**, *2*, 9836–9841. [CrossRef]
36. Wu, S.F.; Li, S.H.; Wang, Y.K.; Huang, C.C.; Sun, Q.; Liang, J.J.; Liao, L.S.; Fung, M.-K. White Organic LED with a Luminous Efficacy Exceeding 100 lm w^{-1} without Light Out-Coupling Enhancement Techniques. *Adv. Funct. Mater.* **2017**, *27*, 1701314. [CrossRef]
37. Jou, J.-H.; Hsieh, C.-Y.; Tseng, J.-R.; Peng, S.-H.; Jou, Y.-C.; Hong, J.H.; Shen, S.-M.; Tang, M.-C.; Chen, P.-C.; Lin, C.-H. Candle Light-Style Organic Light-Emitting Diodes. *Adv. Funct. Mater.* **2013**, *23*, 2750–2757. [CrossRef]
38. Jou, J.-H.; Wu, R.-Z.; Yu, H.-H.; Li, C.-J.; Jou, Y.-C.; Peng, S.-H.; Chen, Y.-L.; Chen, C.-T.; Shen, S.-M.; Joers, P.; et al. Artificial Dusk-Light Based on Organic Light Emitting Diodes. *ACS Photonics* **2014**, *1*, 27–31. [CrossRef]
39. Liu, B.Q.; Wang, L.; Gao, D.Y.; Xu, M.; Zhu, X.H.; Zou, J.H.; Lan, L.F.; Ning, H.L.; Peng, J.B.; Cao, Y. Harnessing charge and exciton distribution towards extremely high performance: The critical role of guests in single-emitting-layer white OLEDs. *Mater. Horiz.* **2015**, *2*, 536–544. [CrossRef]
40. Chen, S.; Qu, Q.; Kong, M.; Zhao, X.; Yu, Z.; Jia, P.; Huang, W. On the Origin of the Shift in Color in White Organic Light-Emitting Diodes. *J. Mater. Chem. C* **2013**, *1*, 3508–3524. [CrossRef]
41. Su, S.-J.; Gonmori, E.; Sasabe, H.; Kido, J. Highly efficient organic blue- and white-light-emitting devices having a carrier- and exciton-confining structure for reduced efficiency roll-off. *Adv. Mater.* **2008**, *20*, 4189–4194. [CrossRef]
42. Zhang, L.; Li, X.; Luo, D.; Xiao, P.; Xiao, W.; Song, Y.; Ang, Q.; Liu, B. Strategies to Achieve High-Performance White Organic Light-Emitting Diodes. *Materials* **2017**, *10*, 1378. [CrossRef] [PubMed]
43. Uoyama, H.; Goushi, K.; Shizu, K.; Nomura, H.; Adachi, C. Highly Efficient Organic Light-Emitting Diodes From Delayed Fluorescence. *Nature* **2012**, *492*, 234–238. [CrossRef] [PubMed]
44. Nishimoto, T.; Yasuda, T.; Lee, S.Y.; Kondo, R.; Adachi, C. A Six-carbazole-decorated Cyclophosphazene as A Host with High Triplet Energy to Realize Efficient Delayed-Fluorescence OLEDs. *Mater. Horiz.* **2014**, *1*, 264–269. [CrossRef]
45. Zhang, Q.; Tsang, D.; Kuwabara, H.; Hatae, Y.; Li, B.; Takahashi, T.; Lee, S.Y.; Yasuda, T.; Adachi, C. Nearly 100% Internal Quantum Efficiency in Undoped Electroluminescent Devices Employing Pure Organic Emitters. *Adv. Mater.* **2015**, *27*, 2096–2100. [CrossRef] [PubMed]

46. Zhang, Q.S.; Li, B.; Huang, S.P.; Nomura, H.; Tanaka, H.; Adachi, C. Efficient blue organic light-emitting diodes employing thermally activated delayed fluorescence. *Nat. Photonics* **2014**, *8*, 326–332. [CrossRef]
47. Wang, H.; Meng, L.Q.; Shen, X.X.; Wei, X.F.; Zheng, X.L.; Lv, X.P.; Yi, Y.P.; Wang, Y.; Wang, P.F. Light-Emitting Diodes: Highly Efficient Orange and Red Phosphorescent Organic Light-Emitting Diodes with Low Roll-Off of Efficiency using a Novel Thermally Activated Delayed Fluorescence Material as Host. *Adv. Mater.* **2015**, *27*, 4041–4047. [CrossRef] [PubMed]
48. Kim, B.S.; Lee, J.Y. Engineering of Mixed Host for High External Quantum Efficiency above 25% in Green Thermally Activated Delayed Fluorescence Device. *Adv. Funct. Mater.* **2015**, *24*, 3970–3977. [CrossRef]
49. Rajamalli, P.; Senthilkumar, N.; Gandeepan, P.; Huang, P.-Y.; Huang, M.-J.; Yang, C.-Y.; Chiu, M.-J.; Chu, L.-K.; Lin, H.-W.; Cheng, C.-H. A New Molecular Design Based on Thermally Activated Delayed Fluorescence for Highly Efficient Organic Light Emitting Diodes. *J. Am. Chem. Soc.* **2016**, *138*, 628–634. [CrossRef] [PubMed]
50. Kim, G.H.; Lampande, R.; Im, J.B.; Lee, J.M.; Lee, J.Y.; Kwon, J.H. Controlling the exciton lifetime of blue thermally activated delayed fluorescence emitters using a heteroatom-containing pyridoindole donor moiety. *Mater. Horiz.* **2017**, *4*, 619–624. [CrossRef]
51. Yang, Z.Y.; Mao, Z.; Xie, Z.L.; Zhang, Y.; Liu, S.W.; Zhao, J.; Xu, J.R.; Chi, Z.G.; Aldred, M.P. Recent advances in organic thermally activated delayed fluorescence materials. *Chem. Soc. Rev.* **2017**, *46*, 915–1016. [CrossRef] [PubMed]
52. Tao, Y.; Yuan, K.; Chen, T.; Xu, P.; Li, H.; Chen, R.; Zheng, C.; Zhang, L.; Huang, W. Thermally activated delayed fluorescence materials towards the breakthrough of organoelectronics. *Adv. Mater.* **2014**, *26*, 7931–7958. [CrossRef] [PubMed]
53. Masui, K.; Nakanotani, H.; Adachi, C. Analysis of exciton annihilation in high-efficiency sky-blue organic light-emitting diodes with thermally activated delayed fluorescence. *Org. Electron.* **2013**, *14*, 2721–2726. [CrossRef]
54. Zhang, D.; Duan, L.; Li, C.; Li, Y.; Li, H.; Zhang, D.; Qiu, Y. High-Efficiency Fluorescent Organic Light-Emitting Devices Using Sensitizing Hosts with a Small Singlet-Triplet Exchange Energy. *Adv. Mater.* **2014**, *26*, 5050–5055. [CrossRef] [PubMed]
55. Nishide, J.-I.; Nakanotani, H.; Hiraga, Y.; Adachi, C. High-efficiency white organic light-emitting diodes using thermally activated delayed fluorescence. *Appl. Phys. Lett.* **2014**, *104*, 233304. [CrossRef]
56. Li, X.L.; Xie, G.Z.; Liu, M.; Chen, D.C.; Cai, X.Y.; Peng, J.B.; Cao, Y.; Su, S.J. High-Efficiency WOLEDs with High Color-Rendering Index based on a Chromaticity-Adjustable Yellow Thermally Activated Delayed Fluorescence Emitter. *Adv. Mater.* **2016**, *28*, 4614–4619. [CrossRef] [PubMed]
57. Mondal, E.; Hung, W.Y.; Dai, H.C.; Wong, K.T. Fluorene-Based Asymmetric Bipolar Universal Hosts for White Organic Light Emitting Devices. *Adv. Funct. Mater.* **2013**, *23*, 3096–3105. [CrossRef]
58. Lee, S.; Shin, H.; Kim, J.J. High-Efficiency Orange and Tandem White Organic Light-Emitting Diodes Using Phosphorescent Dyes with Horizontally Oriented Emitting Dipoles. *Adv. Mater.* **2014**, *26*, 5864–5868. [CrossRef] [PubMed]
59. Fleetham, T.; Huang, L.; Li, J. Tetradentate Platinum Complexes for Efficient and Stable Excimer-Based White OLEDs. *Adv. Funct. Mater.* **2015**, *24*, 6066–6073. [CrossRef]
60. Sun, Y.R.; Giebink, N.C.; Kanno, H.; Ma, B.W.; Thompson, M.E.; Forrest, S.R. Management of Singlet and Triplet Excitons for Efficient White Organic Light-emitting Devices. *Nature* **2006**, *440*, 908–912. [CrossRef] [PubMed]
61. Schwartz, G.; Pfeiffer, M.; Reineke, S.; Walzer, K.; Leo, K. Harvesting Triplet Excitons from Fluorescent Blue Emitters in White Organic Light-Emitting Diodes. *Adv. Mater.* **2007**, *19*, 3672–3676. [CrossRef]
62. Schwartz, G.; Reineke, S.; Rosenow, T.C.; Walzer, K.; Leo, K. Triplet Harvesting in Hybrid White Organic Light-Emitting Diodes. *Adv. Funct. Mater.* **2009**, *19*, 1319–1333. [CrossRef]
63. Ye, J.; Zheng, C.-J.; Ou, X.-M.; Zhang, X.-H.; Fung, M.-K.; Lee, C.-S. Management of Singlet and Triplet Excitons in a Single Emission Layer: A Simple Approach for a High-Efficiency Fluorescence/Phosphorescence Hybrid White Organic Light-Emitting Device. *Adv. Mater.* **2012**, *24*, 3410–3414. [CrossRef] [PubMed]
64. Sun, N.; Wang, Q.; Zhao, Y.B.; Chen, Y.H.; Yang, D.Z.; Zhao, F.C.; Chen, J.S.; Ma, D.G. High-Performance Hybrid White Organic Light-Emitting Devices without Interlayer between Fluorescent and Phosphorescent Emissive Regions. *Adv. Mater.* **2014**, *26*, 1617–1621. [CrossRef] [PubMed]
65. Liu, B.Q.; Nie, H.; Zhou, X.B.; Hu, S.B.; Luo, D.X.; Gao, D.Y.; Zou, J.H.; Xu, M.; Wang, L.; Zhao, Z.J.; et al. Manipulation of Charge and Exciton Distribution Based on Blue Aggregation-Induced Emission Fluorophors:

A Novel Concept to Achieve High-Performance Hybrid White Organic Light-Emitting Diodes. *Adv. Funct. Mater.* **2016**, *26*, 776–783. [CrossRef]
66. Liu, B.Q.; Wang, L.; Gao, D.Y.; Zou, J.H.; Ning, H.L.; Peng, J.B.; Cao, Y. Extremely high-efficiency and ultrasimplified hybrid white organic light-emitting diodes exploiting double multifunctional blue emitting layers. *Light Sci. Appl.* **2016**, *5*, e16137. [CrossRef]
67. Baldo, M.A.; O'Brien, D.F.; Thompson, M.E.; Forrest, S.R. Excitonic Singlet-Triplet Ratio in a Semiconducting Organic Thin Film. *Phys. Rev. B* **1999**, *60*, 14422–14428. [CrossRef]
68. Adachi, C.; Baldo, M.A.; Thompson, M.E.; Forrest, S.R. Nearly 100% Internal Phosphorescence Efficiency in an Organic Light-Emitting Device. *J. Appl. Phys.* **2001**, *90*, 5048–5051. [CrossRef]
69. Zhao, Y.; Zhu, L.; Chen, J.; Ma, D. Improving Color Stability of Blue/Orange Complementary White OLEDs by Using Single-Host Double-Emissive Layer Structure: Comprehensive Experimental Investigation into the Device Working Mechanism. *Org. Electron.* **2012**, *13*, 1340–1348. [CrossRef]
70. Nozoe, S.; Matsuda, M. Enhanced emission by accumulated charges at organic/metal interfaces generated during the reverse bias of organic light emitting diodes. *Appl. Sci.* **2017**, *7*, 1045. [CrossRef]
71. Sang, K.; Kang, L.; Lee, J.E.; Yoo, J.; Yi, Y.; Kwon, H.; Lee, H.; Park, M.H.; Chung, Y. Synthesis and electroluminescence properties of 3-(trifluoromethyl)phenyl-substituted 9,10-diarylanthracene derivatives for blue organic light-emitting diodes. *Appl. Sci.* **2017**, *7*, 1109. [CrossRef]
72. Gao, C.Y.; Chen, K.L.; Sze, P.W.; Ying-Chung Chen, Y.C.; Huang, C.J. Enhancement and Reduction of Nonradiative Decay Process in Organic Light-Emitting Diodes by Gold Nanoparticles. *Appl. Sci.* **2016**, *6*, 441. [CrossRef]
73. Liu, B.; Xu, M.; Wang, L.; Tao, H.; Su, Y.; Gao, D.; Zou, J.; Lan, L.; Peng, J. Comprehensive Study on the Electron Transport Layer in Blue Flourescent Organic Light-Emitting Diodes. *ECS J. Solid State Sci. Technol.* **2015**, *2*, R258–R261. [CrossRef]
74. Ma, Y.; Zhang, H.; Shen, J.; Che, C. Electroluminescence from triplet metal-ligand charge-transfer excited state of transition metal complexes. *Synth. Met.* **1998**, *94*, 245–248. [CrossRef]
75. Baldo, M.A.; O'brien, D.F.; You, Y.; Shoustikov, A.; Sibley, S.; Thompson, M.E.; Forrest, S.R. Highly Efficient Phosphorescent Emission From Organic Electroluminescent Devices. *Nature* **1998**, *395*, 151–154. [CrossRef]
76. Fan, C.; Yang, C. Yellow/orange emissive heavy-metal complexes asphosphors in monochromatic and white organic light-emitting devices. *Chem. Soc. Rev.* **2014**, *43*, 6439–6469. [CrossRef] [PubMed]
77. Seifert, R.; Moraes, I.R.D.; Scholz, S.; Gather, M.C.; Lüssem, B.; Leo, K. Chemical Degradation Mechanisms of Highly Efficient Blue Phosphorescent Emitters Used for Organic Light Emitting Diodes. *Org. Electron.* **2013**, *14*, 115–123. [CrossRef]
78. Liu, B.; Xu, M.; Tao, H.; Ying, L.; Zou, J.; Wu, H.; Peng, J. Highly Efficient Red Phosphorescent Organic Light-Emitting Diodes Based on Solution Processed Emissive Layer. *J. Lumin.* **2013**, *142*, 35–39. [CrossRef]
79. Xiang, C.; Koo, W.; So, F.; Sasabe, H.; Kido, J. A Systematic Study on Efficiency Enhancements in Phosphorescent Green, Red and Blue Microcavity Organic Light Emitting Devices. *Light Sci. Appl.* **2013**, *2*, e74. [CrossRef]
80. Zhang, D.D.; Cai, M.H.; Zhang, Y.G.; Zhang, D.Q.; Duan, L. Sterically Shielded Blue Thermally Activated Delayed Fluorescence Emitters with Improved Efficiency and Stability. *Mater. Horiz.* **2016**, *3*, 145–151. [CrossRef]
81. Liang, Y.; Bing, Y.; Ma, Y.G. Progress in Next-Generation Organic Electroluminescent Materials: Material Design beyond Exciton Statistics. *Sci. Sin. Chim.* **2014**, *57*, 335–345.
82. Kondakov, D.Y. Triplet-triplet Annihilation in Highly Efficient Fluorescent Organic Light-emitting Diodes: Current State and Future Outlook. *Philos. Trans. R. Soc. A* **2015**, *373*, 20140321. [CrossRef] [PubMed]
83. Gray, V.; Dreos, A.; Erhart, P.; Albinsson, B.; Mothpoulsen, K.; Abrahamsson, M. Loss Channels in Triplet-Triplet Annihilation Photon Upconversion: Importance of Annihilator Singlet and Triplet Surface Shapes. *Phys. Chem. Chem. Phys.* **2017**, *19*, 10931–10939. [CrossRef] [PubMed]
84. Shan, T.; Gao, Z.; Tang, X.; He, X.; Gao, Y.; Li, J.; Sun, X.; Liu, Y.; Liu, H.; Yang, B.; et al. Highly Efficient and Stable Pure Blue Nondoped Organic Light-Emitting Diodes at High Luminance Based on Phenanthroimidazole-Pyrene Derivative Enabled by Triplet-Triplet Annihilation. *Dyes Pigment.* **2017**, *142*, 189–197. [CrossRef]
85. Parker, C.A.; Hatchard, C.G. Triplet-singlet emission in fluid solutions. Phosphorescence of eosin. *Trans. Faraday Soc.* **1961**, *57*, 1894–1904. [CrossRef]

86. Blasse, G.; Mcmillin, D.R. On the luminescence of bis (triphenylphosphine) phenanthroline copper(I). *Chem. Phys. Lett.* **1980**, *70*. [CrossRef]
87. Berberan-Santos, M.N.; Garcia, J.M.M. Unusually Strong Delayed Fluorescence of C_{70}. *J. Am. Chem. Soc.* **1996**, *118*, 9391–9394. [CrossRef]
88. Endo, A.; Ogasawara, M.; Takahashi, A.; Yokoyama, D.; Kato, Y.; Adachi, C. Thermally activated delayed fluorescence from $Sn^{(4+)}$-porphyrin complexes and their application to organic light emitting diodes—A novel mechanism for electroluminescence. *Adv. Mater.* **2009**, *21*, 4802–4806. [CrossRef] [PubMed]
89. Zhang, H.; Wang, Z.; Gao, L.; Zhao, B.; Li, W. Low efficiency roll-off and high color stability pure fluorescent white organic light-emitting diode based exciplex host. *RSC Adv.* **2018**, *8*, 954–959. [CrossRef]
90. Jin, W.S.; Lee, J.H.; Moon, C.K.; Kim, K.H.; Shin, H.; Kim, J.J. A fluorescent organic light-emitting diode with 30% external quantum efficiency. *Adv. Mater.* **2014**, *26*, 5684–5688.
91. Osawa, M.; Kawata, I.; Ishii, R.; Igawa, S.; Hashimoto, M.; Hoshino, M. Application of neutral d10 coinage metal complexes with an anionic bidentate ligand in delayed fluorescence-type organic light-emitting diodes. *J. Mater. Chem. C* **2013**, *1*, 4375–4383. [CrossRef]
92. Zink, D.M.; Bächle, M.; Baumann, T.; Nieger, M.; Kühn, M.; Wang, C.; Klopper, W.; Monkowius, U.; Hofbeck, T.; Yersin, H.; et al. Synthesis, Structure and Characterization of Dinuclear Copper(I) Halide Complexes with P^N Ligands Featuring Exciting Photoluminescence Properties. *Inorg. Chem.* **2013**, *52*, 2292–2305. [CrossRef] [PubMed]
93. Augusto, V.; Baleizao, C.; Berberan-Santos, M.N.; Farinha, J. Oxygen-proof fluorescence temperature sensing with pristine C70 encapsulated in polymer nanoparticles. *J. Mater. Chem.* **2010**, *20*, 1192–1197. [CrossRef]
94. Goushi, K.; Yoshida, K.; Sato, K.; Adachi, C. Organic light-emitting diodes employing efficient reverse intersystem crossing for triplet-to-singlet state conversion. *Nat. Photonics* **2012**, *6*, 253–258. [CrossRef]
95. Lee, S.; Kim, K.-H.; Limbach, D.; Park, Y.-S.; Kim, J.-J. Low Roll-Off and High Efficiency Orange Organic Light Emitting Diodes with Controlled Co-Doping of Green and Red Phosphorescent Dopants in an Exciplex Forming Co-Host. *Adv. Funct. Mater.* **2013**, *23*, 4105–4110. [CrossRef]
96. Chapran, M.; Angioni, E.; Findlay, N.J.; Breig, B.; Cherpak, V.; Stakhira, P.; Tuttle, T.; Volyniuk, D.; Grazulevicius, J.V.; Nastishin, Y.A.; et al. An ambipolar BODIPY derivative for a white exciplex OLED and cholesteric liquid crystal laser towards multi-functional devices. *ACS Appl. Mater. Interfaces* **2017**, *9*, 4750–4757. [CrossRef] [PubMed]
97. Cekaviciute, M.; Simokaitiene, J.; Volyniuk, D.; Sini, G.; Grazulevicius, J.V. Arylfluorenyl-substituted metoxytriphenylamines as deep blue exciplex forming bipolar semiconductors for white and blue organic light emitting diodes. *Dyes Pigment.* **2017**, *140*, 187–202. [CrossRef]
98. Luo, D.; Li, X.-L.; Zhao, Y.; Gao, Y.; Liu, B. High-Performance Blue Molecular Emitter-Free and Doping-Free Hybrid White Organic Light-Emitting Diodes: An Alternative Concept to Manipulate Charges and Excitons Based on Exciplex and Electroplex Emission. *ACS Photonics* **2017**, *4*, 1566–1575. [CrossRef]
99. Luo, D.X.; Xiao, Y.; Hao, M.M.; Zhao, Y.; Yang, Y.B.; Gao, Y.; Liu, B.Q. Doping-free white organic light-emitting diodes without blue molecular emitter: An unexplored approach to achieve high performance via exciplex emission. *Appl. Phys. Lett.* **2017**, *110*, 061105. [CrossRef]
100. Yang, Y.; Peng, T.; Ye, K.Q.; Wu, Y.; Liu, Y.; Wang, Y. High-efficiency and high-quality white organic light-emitting diode employing fluorescent emitters. *Org. Electron.* **2011**, *12*, 29–33. [CrossRef]
101. Chuen, C.H.; Tao, Y.T. Highly-bright white organic light-emitting diodes based on a single emission layer. *Appl. Phys. Lett.* **2002**, *81*, 4499–4501. [CrossRef]
102. Liu, B.Q.; Xu, M.; Wang, L.; Su, Y.J.; Gao, D.Y.; Tao, H.; Lan, L.F.; Zou, J.H.; Peng, J.B. High-Performance Hybrid White Organic Light-Emitting Diodes Comprising Ultrathin Blue and Orange Emissive Layers. *Appl. Phys. Express* **2013**, *6*, 122101. [CrossRef]
103. Gather, M.C.; Alle, R.; Becker, H.; Meerholz, K. On the Origin of the Color Shift in White-Emitting OLEDs. *Adv. Mater.* **2007**, *19*, 4460–4465. [CrossRef]
104. Pan, B.; Wang, B.; Wang, Y.; Xu, P.; Wang, L.; Chen, J.; Ma, D. A Simple Carbazole-*N*-Benzimidazole Bipolar Host Material for Highly Efficient Blue and Single Layer White Phosphorescent Organic Light-Emitting Diodes. *J. Mater. Chem. C* **2014**, *2*, 2466–2469. [CrossRef]
105. Liu, B.; Xu, M.; Wang, L.; Yan, X.; Tao, H.; Su, Y.; Gao, D.; Lan, L.; Zou, J.; Peng, J. Investigation and Optimization of Each Organic Layer: A Simple But Effective Approach Towards Achieving High-Efficiency Hybrid White Organic Light-Emitting Diodes. *Org. Electron.* **2014**, *15*, 926–936. [CrossRef]

106. Liu, B.; Wang, L.; Xu, M.; Tao, H.; Xia, X.; Zou, J.; Su, Y.; Gao, D.; Lan, L.; Peng, J. Simultaneous Achievement of Low Efficiency Roll-Off and Stable Color in Highly Efficient Single-Emitting-Layer Phosphorescent White Organic Light-Emitting Diodes. *J. Mater. Chem. C* **2014**, *2*, 5870–5877. [CrossRef]
107. Shao, Y.; Yang, Y. White Organic Light-Emitting Diodes Prepared by a Fused Organic Solid Solution Method. *Appl. Phys. Lett.* **2005**, *86*, 073510. [CrossRef]
108. Wang, Q.; Ding, J.; Ma, D.; Cheng, Y. Highly Efficient Single-Emitting-Layer White Organic Light-Emitting Diodes with Reduced Efficiency Roll-Off. *Appl. Phys. Lett.* **2009**, *94*, 103503. [CrossRef]
109. Liu, B.; Xu, M.; Wang, L.; Tao, H.; Su, Y.; Gao, D.; Lan, L.; Zou, J.; Peng, J. Very-High Color Rendering Index Hybrid White Organic Light-Emitting Diodes with Double Emitting Nanolayers. *Nano-Micro Lett.* **2014**, *6*, 335–339. [CrossRef]
110. Sun, N.; Zhao, Y.B.; Zhao, F.C.; Chen, Y.H.; Yang, D.Z.; Chen, J.S.; Ma, D.G. A white organic light-emitting diode with ultra-high color rendering index, high efficiency and extremely low efficiency roll-off. *Appl. Phys. Lett.* **2014**, *105*, 013303. [CrossRef]
111. Li, X.L.; Ouyang, X.H.; Liu, M.; Ge, Z.Y.; Peng, J.B.; Cao, Y.; Su, S.J. Highly efficient single-and multi-emission-layer fluorescent/phosphorescent hybrid white organic light-emitting diodes with ~20% external quantum efficiency. *J. Mater. Chem. C* **2015**, *3*, 9233–9239. [CrossRef]
112. Ouyang, X.H.; Li, X.L.; Bai, Y.Q.; Mi, D.B.; Ge, Z.Y.; Su, S.J. Highly-efficient hybrid white organic light-emitting diodes based on a high radiative exciton ratio deepblue emitter with improved concentration of phosphorescent dopant. *RSC Adv.* **2015**, *5*, 32298–32306. [CrossRef]
113. Liu, B.Q.; Zou, J.H.; Zhou, Z.W.; Wang, L.; Xu, M.; Tao, H.; Gao, D.Y.; Lan, L.Y.; Ning, H.L.; Peng, J.B. Efficient single-emitting layer hybrid white organic light-emitting diodes with low efficiency roll-off, stable color and extremely high luminance. *J. Ind. Eng. Chem.* **2015**, *30*, 85–91. [CrossRef]
114. Liu, B.Q.; Xu, M.; Tao, H.; Su, Y.J.; Gao, D.Y.; Zou, J.H.; Lan, L.F.; Peng, J.B. The effect of spacer in hybrid white organic light emitting diodes. *Chin. Sci. Bull.* **2014**, *59*, 3090–3097. [CrossRef]
115. Son, Y.H.; Kim, Y.J.; Park, M.J.; Oh, H.Y.; Park, J.S.; Yang, J.H.; Suh, M.C.; Kwon, J.H. Small single–triplet energy gap bipolar host materials for phosphorescent blue and white organic light emitting diodes. *J. Mater. Chem. C* **2013**, *1*, 5008–5014. [CrossRef]
116. Wang, Q.; Ding, J.; Ma, D.; Cheng, Y.; Wang, L.; Jing, X.; Wang, F. Harvesting Excitons Via Two Parallel Channels for Efficient White Organic LEDs with Nearly 100% Internal Quantum Efficiency: Fabrication and Emission Mechanism Analysis. *Adv. Funct. Mater.* **2010**, *19*, 84–95. [CrossRef]
117. Wang, Q.; Ding, J.Q.; Zhang, Z.Q.; Ma, D.G.; Cheng, Y.X.; Wang, L.X.; Wang, F.S. A high-performance tandem white organic light-emitting diode combining highly effective white-units and their interconnection layer. *J. Appl. Phys.* **2009**, *105*, 076101. [CrossRef]
118. Liu, B.Q.; Xu, M.; Wang, L.; Tao, H.; Su, Y.J.; Gao, D.Y.; Lan, L.F.; Zou, J.H.; Peng, J.B. Simplified hybrid white organic light-emitting diodes with efficiency/efficiency roll-off/color rendering index/color-stability trade-off. *Phys. Status Solidi RRL* **2014**, *8*, 719–723. [CrossRef]
119. Wang, Q.; Ding, J.; Ma, D.; Cheng, Y.; Wang, L.; Wang, F. Manipulating Charges and Excitons within a Single-Host System to Accomplish Efficiency/CRI/Color-Stability Trade-off for High-Performance OWLEDs. *Adv. Mater.* **2009**, *21*, 2397–2401. [CrossRef]
120. Chang, Y.L.; Song, Y.; Wang, Z.; Helander, M.G.; Qiu, J.; Chai, L.; Liu, Z.; Scholes, G.D.; Lu, Z. Highly Efficient Warm White Organic Light-Emitting Diodes by Triplet Exciton Conversion. *Adv. Funct. Mater.* **2013**, *23*, 705–712. [CrossRef]
121. Liu, B.Q.; Xu, Z.P.; Zou, J.H.; Tao, H.; Xu, M.; Gao, D.Y.; Lan, L.F.; Wang, L.; Ning, H.L.; Peng, J.B. High-performance hybrid white organic light-emitting diodes employing *p*-type interlayers. *J. Ind. Eng. Chem.* **2015**, *27*, 240–244. [CrossRef]
122. Liu, B.Q.; Tao, H.; Su, Y.J.; Gao, D.Y.; Lan, L.F.; Zou, J.H.; Peng, J.B. Color-stable, reduced efficiency roll-off hybrid white organic light emitting diodes with ultra high brightness. *Chin. Phys. B* **2013**, *22*, 077303. [CrossRef]
123. Zhang, M.; Wang, K.; Zheng, C.-J.; Liu, W.; Lin, H.; Tao, S.-L.; Zhang, X.-H. Efficient, color-stable and high color-rendering-index white organic light-emitting diodes employing full thermally activated delayed fluorescence system. *Org. Electron.* **2017**, *50*, 466–472. [CrossRef]

124. Nakanotani, H.; Higuchi, T.; Furukawa, T.; Masui, K.; Morimoto, K.; Numata, M.; Tanaka, H.; Sagara, Y.; Yasuda, T.; Adachi, C. High-efficiency organic light-emitting diodes with fluorescent emitters. *Nat. Commun.* **2014**, *5*, 4016. [CrossRef] [PubMed]
125. Liao, X.; Yang, X.; Cheng, J.; Li, Y.; Meng, X.; Li, J.; Pei, Q.; Li, L. Solution processed warm white organic light-emitting diodes based on a blue thermally activated delayed fluorescent dendrimer. *Chem. Plus. Chem.* **2018**. [CrossRef]
126. Higuchi, T.; Nakanotani, H.; Adachi, C. High-Efficiency White Organic Light-Emitting Diodes Based on a Blue Thermally Activated Delayed Fluorescent Emitter Combined with Green and Red Fluorescent Emitters. *Adv. Mater.* **2015**, *27*, 2019–2023. [CrossRef] [PubMed]
127. Liu, B.Q.; Wang, L.; Zou, J.H.; Tao, H.; Su, Y.J.; Gao, D.Y.; Xu, M.; Lan, L.F.; Peng, J.B. Investigation on spacers and structures: A simple but effective approach toward high-performance hybrid white organic light emitting diodes. *Synth. Met.* **2013**, *184*, 5–9. [CrossRef]
128. Liu, B.Q.; Zou, J.H.; Su, Y.J.; Gao, D.Y.; Lan, L.F.; Tao, H.; Peng, J.B. Hybrid white organic light emitting diodes with low efficiency roll-off, stable color and extreme brightness. *J. Lumin.* **2014**, *151*, 161–164. [CrossRef]
129. Liu, B.Q.; Tao, H.; Wang, L.; Gao, D.Y.; Liu, W.C.; Zou, J.H.; Xu, M.; Ning, H.L.; Peng, J.B.; Cao, Y. High-performance doping-free hybrid white organic light-emitting diodes: The exploitation of ultrathin emitting nanolayers (<1 nm). *Nano Energy* **2016**, *26*, 26–36. [CrossRef]
130. Schwartz, G.; Fehse, K.; Pfeiffer, M.; Walzer, K.; Leo, K. Highly efficient white organic light emitting diodes comprising an interlayer to separate fluorescent and phosphorescent regions. *Appl. Phys. Lett.* **2006**, *89*, 083509. [CrossRef]
131. Luo, D.X.; Yang, Y.F.; Xiao, Y.; Zhao, Y.; Yang, Y.B.; Liu, B.Q. Regulating Charge and Exciton Distribution in High-Performance Hybrid White Organic Light-Emitting Diodes with *n*-Type Interlayer Switch. *Nano-Micro Lett.* **2017**, *9*, 37. [CrossRef]
132. Lee, S.Y.; Yasuda, T.; Yang, Y.S.; Zhang, Q.; Adachi, C. Luminous Butterflies: Efficient Exciton Harvesting by Benzophenone Derivatives for Full-Color Delayed Fluorescence OLEDs. *Angew. Chem.* **2014**, *126*, 6520–6524. [CrossRef]
133. Chen, J.; Zhao, F.; Ma, D. Hybrid White OLEDs with Fluorophors and Phosphors. *Mater. Today* **2014**, *17*, 175–183. [CrossRef]
134. Liu, B.Q.; Luo, D.X.; Zou, J.H.; Gao, D.Y.; Ning, H.L.; Wang, L.; Peng, J.B.; Cao, Y. A host-guest system comprising high guest concentration to achieve simplified and high-performance hybrid white organic light-emitting diodes. *J. Mater. Chem. C* **2015**, *3*, 6359–6366. [CrossRef]
135. Liu, B.Q.; Xu, M.; Wang, L.; Zou, J.H.; Tao, H.; Su, Y.J.; Gao, D.Y.; Ning, H.L.; Lan, L.F.; Peng, J.B. Regulating charges and excitons in simplified hybrid white organic light-emitting diodes: The key role of concentration in single dopant host-guest systems. *Org. Electron.* **2014**, *15*, 2616–2623. [CrossRef]
136. Zhao, B.; Zhang, T.Y.; Li, W.L.; Su, Z.S.; Chu, B.; Yan, X.W.; Jin, F.M.; Gao, Y.; Wu, H. Organic Electronics Highly efficient and color stable single-emitting-layer fluorescent WOLEDs with delayed fluorescent host. *Org. Electron.* **2015**, *23*, 208–212. [CrossRef]
137. Song, W.; Lee, I.H.; Hwang, S.H.; Lee, J.Y. High efficiency fluorescent white organic light-emitting diodes having a yellow fluorescent emitter sensitized by a blue thermally activated delayed fluorescent emitter. *Org. Electron.* **2015**, *23*, 138–143. [CrossRef]
138. Song, W.; Lee, I.; Lee, J.Y. Host engineering for high quantum efficiency blue and white fluorescent organic light-emitting diodes. *Adv. Mater.* **2015**, *27*, 4358–4363. [CrossRef] [PubMed]
139. Zhang, D.D.; Duan, L.; Zhang, Y.G.; Cai, M.H.; Zhang, D.Q.; Qiu, Y. Highly efficient hybrid warm white organic light-emitting diodes using a blue thermally activated delayed fluorescence emitter: Exploiting the external heavy-atom effect. *Light Sci. Appl.* **2015**, *4*, e232. [CrossRef]
140. Zhang, D.D.; Zhang, D.Q.; Duan, L. Exploiting *p*-Type Delayed Fluorescence in Hybrid White OLEDs: Breaking the Trade-off between High Device Efficiency and Long Lifetime. *ACS Appl. Mater. Interfaces* **2016**, *8*, 23197–23203. [CrossRef] [PubMed]
141. Kim, M.; Jeon, S.K.; Hwang, S.H.; Lee, J.Y. Stable Blue Thermally Activated Delayed Fluorescent Organic Light-Emitting Diodes with Three Times Longer Lifetime than Phosphorescent Organic Light-Emitting Diodes. *Adv. Mater.* **2015**, *27*, 2515–2520. [CrossRef] [PubMed]

142. Zhang, D.D.; Duan, L.; Li, Y.L.; Zhang, D.Q.; Qiu, Y. Highly efficient and color-stable hybrid warm white organic light-emitting diodes using a blue material with thermally activated delayed fluorescence. *J. Mater. Chem. C* **2014**, *2*, 8191–8197. [CrossRef]
143. Chen, Y.; Zhao, F.; Zhao, Y.; Chen, J.; Ma, D. Ultra-simple hybrid white organic light-emitting diodes with high efficiency and CRI trade-off: Fabrication and emission-mechanism analysis. *Org. Electron.* **2012**, *13*, 2807–2815. [CrossRef]
144. Zheng, C.-J.; Wang, J.; Ye, J.; Lo, M.-F.; Liu, X.-K.; Fung, M.-K.; Zhang, X.-H.; Lee, C.-S. Novel Efficient Blue Fluorophors with Small Singlet-Triplet Splitting: Hosts for Highly Efficient Fluorescence and Phosphorescence Hybrid WOLEDs with Simplified Structure. *Adv. Mater.* **2013**, *25*, 2205–2211. [CrossRef] [PubMed]
145. Chen, P.; Xie, W.F.; Li, K.; Guan, T.; Duan, Y.; Zhao, Y.; Liu, S.Y.; Ma, C.S.; Zhang, L.Y.; Li, B. White organic light-emitting devices with a bipolar transport layer between blue fluorescent and orange phosphorescent emitting layers. *Appl. Phys. Lett.* **2007**, *91*, 023505. [CrossRef]
146. Zhang, L.J.; Hua, Y.L.; Wu, X.M.; Wang, Y.; Yin, S.G. White organic light-emitting device with both phosphorescent and fluorescent emissive layers. *Chin. Phys. B* **2008**, *17*, 3097.
147. Ho, C.L.; Wong, W.Y.; Wang, Q.; Ma, D.G.; Wang, L.X.; Lin, Z.Y. Multifunctional Iridium-Carbazolyl Orange Phosphor for HighPerformance Two-Element WOLED Exploiting Exciton-Managed Fluorescence/Phosphorescence. *Adv. Funct. Mater.* **2008**, *18*, 928–937. [CrossRef]
148. Peng, Q.M.; Chen, P.; Sun, J.X.; Li, F. Magnetic field effects on electroluminescence emanated simultaneously from blue fluorescent and red phosphorescent emissive layers of an organic light-emitting diode. *Org. Electron.* **2012**, *13*, 3040–3044. [CrossRef]
149. Zhao, F.C.; Zhang, Z.Q.; Liu, Y.P.; Dai, Y.F.; Chen, J.S.; Ma, D.G. A hybrid white organic light-emitting diode with stable color and reduced efficiency roll-off by using a bipolar charge carrier switch. *Org. Electron.* **2012**, *13*, 1049–1055. [CrossRef]
150. Zhao, F.C.; Chen, Y.H.; Wang, Q.; Ma, D.G. Studies of fluorescence/phosphorescence hybrid white organic light-emitting diodes. *Sci. Sin. Chim.* **2013**, *43*, 398–406. [CrossRef]
151. Schwartz, G.; Ke, T.-H.; Wu, C.-C.; Walzer, K.; Leo, K. Balanced ambipolar charge carrier mobility in mixed layers for application in hybrid white organic light-emitting diodes. *Appl. Phys. Lett.* **2008**, *93*, 073304. [CrossRef]
152. Schwartz, G.; Reineke, S.; Walzer, K.; Leo, K. Reduced efficiency roll-off in high-efficiency hybrid white organic light-emitting diodes. *Appl. Phys. Lett.* **2008**, *92*, 053311. [CrossRef]
153. Liu, B.Q.; Wang, L.; Xu, M.; Tao, H.; Zou, J.H.; Gao, D.Y.; Lan, L.F.; Ning, H.L.; Peng, J.B.; Cao, Y. Efficient Hybrid White Organic Light-emitting Diodes with Extremely Long Lifetime: The Effect of *n*-type Interlayer. *Sci. Rep.* **2014**, *4*, 7198. [CrossRef] [PubMed]
154. Wu, Z.B.; Luo, J.J.; Sun, N.; Zhu, L.P.; Sun, H.D.; Yu, L.; Yang, D.Z.; Qiao, X.F.; Chen, J.S.; Yang, C.L.; et al. High Performance Hybrid White Organic Light-Emitting Diodes with Superior Efficiency/Color Rendering Index/Color Stability and Low Efficiency Roll-Off Based on a Blue Thermally Activated Delayed Fluorescent Emitter. *Adv. Funct. Mater.* **2016**, *26*, 3306–3313. [CrossRef]
155. Luo, D.X.; Yang, Y.B.; Huang, L.; Liu, B.Q.; Zhao, Y. High-performance hybrid white organic light-emitting diodes exploiting blue thermally activated delayed fluorescent dyes. *Dyes Pigment.* **2017**, *147*, 83–89. [CrossRef]
156. Song, W.; Lee, J.Y. High-power-efficiency hybrid white organic light-emitting diodes with a single emitting layer doped with blue delayed fluorescent and yellow phosphorescent emitters. *J. Phys. D Appl. Phys.* **2015**, *48*, 365106. [CrossRef]
157. Chen, Z.; Liu, X.K.; Zheng, C.J.; Ye, J.; Liu, C.L.; Li, F.; Ou, X.M.; Lee, C.S.; Zhang, X.H. High Performance Exciplex-Based Fluorescence-Phosphorescence White Organic Light-Emitting Device with Highly Simplified Structure. *Chem. Mater.* **2015**, *27*, 5206–5211. [CrossRef]
158. Hung, W.Y.; Fang, G.C.; Lin, S.W.; Cheng, S.H.; Wong, K.T.; Kuo, T.Y.; Chou, P.T. The First Tandem, All-exciplex-based WOLED. *Sci. Rep.* **2014**, *4*, 5161. [CrossRef] [PubMed]
159. Zhang, D.; Cao, X.; Wu, Q.; Zhang, M.; Sun, N.; Zhang, X.; Tao, Y. Purely organic materials for extremely simple all-tadf white OLEDs: A new carbazole/oxadiazole hybrid material as a dual-role non-doped light blue emitter and highly efficient orange host. *J. Mater. Chem. C* **2018**. [CrossRef]

160. Meng, L.; Wang, H.; Wei, X.; Lv, X.; Wang, Y.; Wang, P. White light emitting diodes based on a yellow thermally activated delayed fluorescent emitter and blue fluorescent emitter. *RSC Adv.* **2015**, *5*, 59137–59141. [CrossRef]
161. Zhao, B.; Zhang, T.; Chu, B.; Li, W.; Su, Z.; Luo, Y.; Li, R.; Yan, X.; Jin, F.; Gao, Y.; Wu, H. Highly efficient tandem full exciplex orange and warm white OLEDs based on thermally activated delayed fluorescence mechanism. *Org. Electron.* **2015**, *17*, 15–21. [CrossRef]
162. Liu, X.-K.; Zhan, C.; Jian, Q.; Wen-Jun, Z.; Bo, W.; Hoi Lam, T.; Zhu, F.; Zhang, X.-H.; Lee, C.-S. Organic light-emitting devices: Remanagement of singlet and triplet excitons in single-emissive-layer hybrid white organic light-emitting devices using thermally activated delayed fluorescent blue exciplex. *Adv. Mater.* **2015**, *27*, 7079–7085. [CrossRef] [PubMed]
163. Kim, H.G.; Kim, K. H.; Moon, C. K.; Kim, J.J. Harnessing triplet excited states by fluorescent dopant utilizing codoped phosphorescent dopant in exciplex host for effcient fluorescent organic light emitting diodes. *Adv. Optical Mater.* **2017**, *5*, 1600749. [CrossRef]
164. Zhang, T.; Zhao, B.; Chu, B.; Li, W.; Su, Z.; Yan, X.; Liu, C.; Wu, H.; Gao, Y.; Jin, F.; et al. Simple structured hybrid WOLEDs based on incomplete energy transfer mechanism: From blue exciplex to orange dopant. *Sci. Rep.* **2015**, *5*, 10234. [CrossRef] [PubMed]
165. Liu, W.; Zheng, C.J.; Wang, K.; Zhang, M.; Chen, D.Y.; Tao, S.L.; Li, F.; Dong, Y.-P.; Lee, C.-S.; Ou, X.-M.; et al. High performance all fluorescence white organic light emitting devices with a highly simplified structure based on thermally activated delayed fluorescence dopants and host. *ACS Appl. Mater. Interfaces* **2016**, *8*, 32984–32991. [CrossRef] [PubMed]
166. Kim, B.S.; Yook, K.S.; Lee, J.Y. Above 20% External Quantum Efficiency in Novel Hybrid White Organic Light-Emitting Diodes Having Green Thermally Activated Delayed Fluorescent Emitter. *Sci. Rep.* **2014**, *4*, 6019168. [CrossRef] [PubMed]
167. Yong, J.C.; Yook, K.S.; Lee, J.Y. Cool and Warm Hybrid White Organic Light-Emitting Diode with Blue Delayed Fluorescent Emitter Both as Blue Emitter and Triplet Host. *Sci. Rep.* **2015**, *5*, 7859. [CrossRef]
168. Wu, Z.; Qi, W.; Ling, Y.; Chen, J.; Qiao, X.; Ahamad, T.; Alshehri, S.M.; Yang, C.; Ma, D. Managing excitons and charges for high-performance fluorescent white organic light-emitting diodes. *Acs Appl. Mater. Interfaces* **2016**, *8*, 28780–28788. [CrossRef] [PubMed]
169. Sasabe, H.; Takamatsu, J.; Motoyama, T.; Watanabe, S.; Wagenblast, G.; Langer, N.; Molt, O.; Fuchs, E.; Lennartz, C.; Kido, J. High-Efficiency Blue and White Organic Light-Emitting Devices Incorporating a Blue Iridium Carbene Complex. *Adv. Mater.* **2010**, *22*, 5003–5007. [CrossRef] [PubMed]
170. Shi, C.; Sun, N.; Wu, Z.; Chen, J.; Ahamad, T.; Alshehri, S.M.; Ma, D. Managing excitons for high performance hybrid white organic light-emittingdiodes by using a simple planar heterojunction interlayer. *Appl. Phys. Lett.* **2018**, *112*, 023301. [CrossRef]
171. Wu, Z.; Yu, L.; Zhao, F.; Qiao, X.; Chen, J.; Ni, F.; Yang, C.; Ahamad, T.; Alshehri, S.M.; Ma, D. Precise Exciton Allocation for Highly Effcient White Organic Light-Emitting Diodes with Low Effciency Roll-Off Based on Blue Thermally Activated Delayed Fluorescent Exciplex Emission. *Adv. Opt. Mater.* **2017**, *5*, 1700415. [CrossRef]
172. Yoshihiro, O. Color rendering and luminous efficacy of white LED spectra. *Proc. SPIE* **2004**, *88*, 5530. [CrossRef]
173. Wang, Q.; Oswald, I.W.H.; Yang, X.L.; Zhou, G.J.; Jia, H.P.; Qiao, Q.Q.; Chen, Y.H.; Jason, H.-H.; Gnade, B.E. A Non-Doped Phosphorescent Organic Light-Emitting Device with Above 31% External Quantum Efficiency. *Adv. Mater.* **2014**, *26*, 8107–8113. [CrossRef] [PubMed]
174. Poloek, A.; Chen, C.-T.; Chen, C.-T. High performance hybrid white and multi-colour electroluminescence from a new host material for a heteroleptic naphthyridinolate platinum complex dopant. *J. Mater. Chem. C* **2014**, *2*, 1376–1380. [CrossRef]
175. Sun, N.; Wang, Q.; Zhao, Y.B.; Yang, D.Z.; Zhao, F.C.; Chen, J.S.; Ma, D.G. A hybrid white organic light-emitting diode with above 20% external quantum efficiency and extremely low efficiency roll-off. *J. Mater. Chem. C* **2014**, *2*, 7494–7504. [CrossRef]
176. Kim, S.Y.; Jeong, W.I.; Mayr, C.; Park, Y.S.; Kim, K.H.; Lee, J.H.; Moon, C.K.; Brütting, W.; Kim, J.J. Organic Light-Emitting Diodes with 30% External Quantum Efficiency Based on a Horizontally Oriented Emitter. *Adv. Funct. Mater.* **2013**, *23*, 3896–3900. [CrossRef]

177. Chen, Y.-H.; Dong-Ge Ma, D.-G.; Sun, H.-D.; Chen, J.-S.; Guo, Q.-X.; Wang, Q.; Zhao, Y.-B. Organic Semiconductor Heterojunctions: Electrode-Independent Charge Injectors for High-Performance Organic Light-Emitting Diodes. *Light Sci. Appl.* **2016**, *5*, e16042. [CrossRef]
178. Gomez, E.F.; Steckl, A.J. Improved Performance of OLEDs on Cellulose/Epoxy Substrate Using Adenine as a Hole Injection Layer. *ACS Photonics* **2015**, *2*, 439–445. [CrossRef]
179. Liu, B.; Lan, L.; Zou, J.; Peng, J. A novel organic light-emitting diode by utilizing double hole injection layer. *Acta Phys. Sin.* **2013**, *62*, 087302. [CrossRef]
180. Hong, T.; Gao, D.; Liu, B.; Wang, L.; Zou, J.; Xu, M.; Peng, J. Enhancement of tandem organic light-emitting diode performance by inserting an ultra-thin Ag layer in charge generation layer. *Acta Phys. Sin.* **2017**, *1*, 017302. [CrossRef]
181. Reineke, S.; Lindner, F.; Schwartz, G.; Seidler, N.; Walzer, K.; Lüssem, B.; Leo, K. White organic light-emitting diodes with fluorescent tube efficiency. *Nature* **2009**, *459*, 234. [CrossRef] [PubMed]
182. Kim, D.Y.; Park, J.H.; Lee, J.W.; Hwang, S.; Oh, S.J.; Kim, J.; Sone, C.; Schubert, E.F.; Kim, J.K. Overcoming the fundamental light-extraction efficiency limitations of deep ultraviolet light-emitting diodes by utilizing transverse-magnetic-dominant emission. *Light Sci. Appl.* **2015**, *4*, e263. [CrossRef]
183. Preinfalk, J.B.; Eiselt, T.; Wehlus, T.; Rohnacher, V.; Hanemann, T.; Gomard, G.; Lemmer, U. Large-Area Screen-Printed Internal Extraction Layers for Organic Light-Emitting Diodes. *ACS Photonics* **2017**, *4*, 928–933. [CrossRef]
184. Koh, T.-W.; Spechler, J.A.; Lee, K.M.; Arnold, C.B.; Rand, B.P. Enhanced Outcoupling in Organic Light-Emitting Diodes via a High-Index Contrast Scattering Layer. *ACS Photonics* **2015**, *2*, 1366–1372. [CrossRef]
185. Yook, K.S.; Jeon, S.O.; Min, S.Y.; Lee, J.Y.; Yang, H.J.; Noh, T.; Kang, S.K.; Lee, T.W. Highly Efficient p-i-n and Tandem Organic Light-Emitting Devices Using an Air-Stable and Low-Temperature-Evaporable Metal Azide as an *n*-Dopant. *Adv. Funct. Mater.* **2010**, *20*, 1797–1802. [CrossRef]
186. Sun, H.D.; Guo, Q.X.; Yang, D.Z.; Chen, Y.H.; Chen, J.S.; Ma, D.G. High Efficiency Tandem Organic Light Emitting Diode Using an Organic Heterojunction as the Charge Generation Layer: An Investigation into the Charge Generation Model and Device Performance. *ACS Photonics* **2015**, *2*, 271–279. [CrossRef]
187. Ding, L.; Sun, Y.Q.; Chen, H.; Zu, F.S.; Wang, Z.K.; Liao, L.S. A novel intermediate connector with improved charge generation and separation for large-area tandem white organic lighting devices. *J. Mater. Chem. C* **2014**, *2*, 10403–10408. [CrossRef]
188. Chang, C.C.; Chen, J.F.; Hwang, S.W.; Chen, C.H. Highly efficient white organic electroluminescent devices based on tandem architecture. *Appl. Phys. Lett.* **2005**, *87*, 253501. [CrossRef]
189. Guo, F.; Ma, D. White organic light-emitting diodes based on tandem structures. *Appl. Phys. Lett.* **2005**, *87*, 173510. [CrossRef]
190. Gong, S.; Chen, Y.; Luo, J.; Yang, C.; Zhong, C.; Qin, J.; Ma, D. Bipolar Tetraarylsilanes as Universal Hosts for Blue, Green, Orange and White Electrophosphorescence with High Efficiency and Low Efficiency Roll-Off. *Adv. Funct. Mater.* **2011**, *21*, 1168–1178. [CrossRef]
191. Huang, W.Y.; Chen, Z.W.; You, H.W.; Fan, F.C.; Chen, H.F.; Wong, K.T. Efficient carrier- and exciton-confining device structure that enhances blue PhOLED efficiency and reduces efficiency roll-off. *Org. Electron.* **2011**, *12*, 575–581. [CrossRef]
192. D'Andrade, B.W.; Holmes, R.J.; Forrest, S.R. Efficient Organic Electrophosphorescent White-Light-Emitting Device with a Triple Doped Emissive Layer. *Adv. Mater.* **2004**, *16*, 624–628. [CrossRef]
193. Guo, J.J.; Li, X.L.; Nie, H.; Luo, W.W.; Gan, S.F.; Hu, S.M.; Hu, R.R.; Qin, A.J.; Zhao, Z.J.; Su, S.J.; et al. Achieving High-Performance Nondoped OLEDs with Extremely Small Efficiency Roll-Off by Combining Aggregation-Induced Emission and Thermally Activated Delayed Fluorescence. *Adv. Funct. Mater.* **2017**, *27*, 1606458. [CrossRef]
194. Duan, L.; Zhang, D.Q.; Wu, K.W.; Huang, X.Q.; Wang, L.D.; Qiu, Y. Controlling the Recombination Zone of White Organic Light-Emitting Diodes with Extremely Long Lifetimes. *Adv. Funct. Mater.* **2011**, *21*, 3540–3545. [CrossRef]
195. Xue, K.W.; Han, G.G.; Duan, Y.; Chen, P.; Yang, Y.Q.; Yang, D.; Duan, Y.H.; Wang, X.; Zhao, Y. Doping-free orange and white phosphorescent organic light-emitting diodes with ultra-simply structure and excellent color stability. *Org. Electron.* **2015**, *18*, 84–88. [CrossRef]

196. Chen, S.; Zhao, X.; Wu, Q.; Shi, H.; Mei, Y.; Zhang, R.; Wang, L.; Huang, W. Efficient, Color-Stable Flexible White Top-Emitting Organic Light-Emitting Diodes. *Org. Electron.* **2013**, *14*, 3037–3045. [CrossRef]
197. Du, X.Y.; Tao, S.L.; Huang, Y.; Yang, X.X.; Ding, X.L.; Zhang, X.H. Efficient fluorescence/phosphorescence white organic light-emitting diodes with ultra high color stability and mild efficiency roll-off. *Appl. Phys. Lett.* **2015**, *107*, 183304. [CrossRef]
198. Yook, K.S.; Jeon, S.O.; Joo, C.W.; Lee, J.Y. Color stability and suppressed efficiency roll-off in white organic light-emitting diodes through management of interlayer and host properties. *J. Ind. Eng. Chem.* **2009**, *15*, 420–422. [CrossRef]
199. Fröbel, M.; Schwab, T.; Kliem, M.; Hofmann, S.; Leo, K.; Gather, M.C. Get It White: Color-Tunable Ac/Dc OLEDs. *Light Sci. Appl.* **2015**, *4*, e247. [CrossRef]
200. Aizawa, N.; Pu, Y.J.; Watanabe, M.; Chiba, T.; Ideta, K.; Toyota, N.; Igarashi, M.; Suzuri, Y.; Sasabe, H.; Kido, J. Solution-Processed Multilayer Small-Molecule Light-Emitting Devices with High-Efficiency White-Light Emission. *Nat. Commun.* **2014**, *5*, 5756. [CrossRef] [PubMed]
201. Hou, L.; Duan, L.; Qiao, J.; Zhang, D.; Dong, G.; Wang, L.; Qiu, Y. Efficient Solution-Processed Small-Molecule Single Emitting Layer Electrophosphorescent White Light-Emitting Diodes. *Org. Electron.* **2010**, *11*, 1344–1350. [CrossRef]
202. Zou, J.; Wu, H.; Lam, C.S.; Wang, C.; Zhu, J.; Zhong, C.; Hu, S.; Ho, C.L.; Zhou, G.J.; Wu, H.B.; et al. Simultaneous Optimization of Charge-Carrier Balance and Luminous Efficacy in Highly Efficient White Polymer Light-Emitting Devices. *Adv. Mater.* **2011**, *23*, 2976–2980. [CrossRef] [PubMed]
203. Jiang, C.; Zhong, Z.; Liu, B.; He, Z.; Zou, J.; Wang, L.; Wang, J.; Peng, J.B.; Cao, Y. Coffee-Ring-Free Quantum Dot Thin Film Using Inkjet Printing from a Mixed-Solvent System on Modified ZnO Transport Layer for Light-Emitting Devices. *ACS Appl. Mater. Interfaces* **2016**, *8*, 26162–26168. [CrossRef] [PubMed]
204. Wang, Q.; Oswald, I.W.H.; Perez, M.R.; Jia, H.P.; Shahub, A.A.; Qiao, Q.Q.; Gnade, B.E.; Omary, M.A. Doping-Free Organic Light-Emitting Diodes with Very High Power Efficiency, Simple Device Structure and Superior Spectral Performance. *Adv. Funct. Mater.* **2014**, *24*, 4746–4752. [CrossRef]
205. Zhao, Y.B.; Chen, J.S.; Ma, D.G. Ultrathin Nondoped Emissive Layers for Efficient and Simple Monochrome and White Organic Light-Emitting Diodes. *ACS Appl. Mater. Interfaces* **2013**, *5*, 965–971. [CrossRef] [PubMed]
206. Liu, B.; Nie, H.; Lin, G.; Hu, S.; Gao, D.; Zou, J.; Xu, M.; Wang, L.; Zhao, Z.; Ning, H.; et al. High-Performance Doping-Free Hybrid White OLEDs Based on Blue Aggregation-Induced Emission Luminogens. *ACS Appl. Mater. Interfaces* **2017**, *9*, 34162–34171. [CrossRef] [PubMed]
207. Liu, B.; Wang, L.; Tao, H.; Xu, M.; Zou, J.; Ning, H.; Peng, J.; Cao, Y. Doping-Free Tandem White Organic Light-Emitting Diodes. *Sci. Bull.* **2017**, *62*, 1193–1200. [CrossRef]
208. Cherpak, V.; Stakhira, P.; Minaev, B.; Baryshnikov, G.; Stromylo, E.; Helzhynskyy, I.; Chapran, M.; Volyniuk, D.; Hotra, Z.; Dabuliene, A.; et al. Mixing of Phosphorescent and Exciplex Emission in Efficient Organic Electroluminescent Devices. *ACS Appl. Mater. Interfaces* **2015**, *7*, 1219–1225. [CrossRef] [PubMed]
209. Krotkus, S.; Kasemann, D.; Lenk, S.; Leo, K.; Reineke, S. Adjustable White-Light Emission From a Photo-Structured Micro-OLED Array. *Light Sci. Appl.* **2016**, *5*, e16121. [CrossRef]
210. Guan, N.; Dai, X.; Messanvi, A.; Zhang, H.; Yan, J.; Gautier, E.; Bougerol, C.; Julien, F.H.; Durand, C.; Eyery, J.; et al. Flexible White Light Emitting Diodes Based on Nitride Nanowires and Nanophosphors. *ACS Photonics* **2016**, *3*, 597–603. [CrossRef] [PubMed]